sustainability

MDPI

Review

The Influence of Gas Fuel Enrichment with Hydrogen on the Combustion Characteristics of Combustors: A Review

Rabeea M. Ghazal [1], Abdulrazzak Akroot [1], Hasanain A. Abdul Wahhab [2,*], Abdulrahman E. J. Alhamd [1], Ameer Hasan Hamzah [1] and Mothana Bdaiwi [1]

[1] Department of Mechanical Engineering, Faculty of Engineering, Karabük University, Karabük 78050, Turkey; rabeaagazal@gmail.com (R.M.G.); abdulrazzakakroot@karabuk.edu.iq (A.A.); ej.abdrahman@gmail.com (A.E.J.A.); ameer.hassan@uta.edu.iq (A.H.H.); mothna777@gmail.com (M.B.)
[2] Training and Workshop Centre, University of Technology-Iraq, Baghdad 35050, Iraq
* Correspondence: 20085@uotechnology.edu.iq

Abstract: Hydrogen is a promising fuel because it has good capabilities to operate gas turbines. Due to its ignition speed, which exceeds the ignition of traditional fuel, it achieves a higher thermal efficiency while the resulting emissions are low. So, it was used as a clean and sustainable energy source. This paper reviews the most important research that was concerned with studying the characteristics of hydrogen combustion within incinerators and power generation equipment, where hydrogen was used as a fuel mixed with traditional fuel in the combustion chambers of gas turbines. It also includes an evaluation of the combustion processes and flame formation resulting from the enrichment of gaseous fuels with hydrogen and partial oxidation. A large amount of theoretical and experimental work in this field has been reviewed. This review summarizes the predictive and experimental results of various research interests in the field of hydrogen combustion and also production.

Keywords: hydrogen; fuel flexible combustor; natural gas–hydrogen blend; laminar burning velocity

check for updates

Citation: Ghazal, R.M.; Akroot, A.; Abdul Wahhab, H.A.; Alhamd, A.E.J.; Hamzah, A.H.; Bdaiwi, M. The Influence of Gas Fuel Enrichment with Hydrogen on the Combustion Characteristics of Combustors: A Review. *Sustainability* **2024**, *16*, 9423. https://doi.org/10.3390/su16219423

Received: 29 July 2024
Revised: 16 October 2024
Accepted: 20 October 2024
Published: 30 October 2024

Copyright: © 2024 by the authors. Licensee MDPI, Basel, Switzerland. This article is an open access article distributed under the terms and conditions of the Creative Commons Attribution (CC BY) license (https://creativecommons.org/licenses/by/4.0/).

1. Introduction

The use of lean hydrocarbon combustion in various types of combustors, such as the burners of boilers, furnaces, and the combustion chambers of gas turbines and internal combustion engines, has benefits in terms of reduced emissions of CO, NOx, and unburned hydrocarbons. Additionally, it leads to an improved economy for fuel. Interestingly, the combustion of the hydrocarbon/air mixture on the lean sides has been observed to have difficulty igniting. Its flammability is very low in this region (with an equivalence ratio of less than 1.0). More so, the results of the lack of combustion and increased levels of unburned hydrocarbons ultimately lead to decreased performance and decreased fuel economy [1]. Additionally, maintaining a stable flame in the lean hydrocarbon mixtures can be difficult, leading to a malfunction of the combustors [2]. In order to enhance environmental performance, combustion engines today can be converted to run on alternative fuels that result in lower emissions. This approach requires the use and development of technology through which zero emissions can be achieved. Hydrogen is emerging as one of the most promising possibilities in this regard. In the nineteenth century, experiments were performed using a series of successful steam-powered carriage designs. The experiments included the main goal of keeping the engine running continuously by causing an internal explosion in the cylinder, using a mixture of oxygen and hydrogen gases at that time to start this combustion, and the results showed great success [3]. Car manufacturers, academic institutions, inventors, and enthusiasts all examined the feasibility of hydrogen-powered combustion engines further during the 20th century. Paul Dieges obtained a patent in 1970 for a modified internal combustion engine that enabled conventional gasoline-powered engines to operate on hydrogen fuel [4–7].

Hydrogen combustion investigations refer to the study of the combustion process of hydrogen gas, which is a highly flammable and energy-rich gas. Combustion is a chemical reaction between a fuel (in this case, hydrogen) and an oxidizer (usually oxygen) that results in the release of heat, energy, and products (water and CO_2). Hydrogen combustion has been a topic of significant interest due to hydrogen's potential as a sustainable and renewable energy carrier, as it produces only water vapor when burned and releases a minimum level of harmful greenhouse gas emissions or air pollutants. Hydrogen combustion investigations can cover a wide range of topics, including fundamental combustion chemistry, combustion kinetics, flame structure, ignition characteristics, flame stability, and reducing pollutants. These investigations may be conducted through experimental, computational, or theoretical approaches, or a combination of these methods [8]. Experimental investigations of hydrogen combustion often involve the use of specialized combustion chambers or test rigs to simulate real-world combustion conditions. In general, these works have covered the combustion of hydrogen alone as well as testing it in combination with various conventional fuels.

Measurements of the temperature, pressure, species concentrations, and flame properties are commonly collected using instruments such as thermocouples, pressure transducers, gas analyzers, and spectroscopic techniques [9]. Experimental investigations can provide valuable data for validating combustion models, understanding reaction pathways, and characterizing combustion behavior under different conditions. Computational investigations of hydrogen combustion typically involve the use of computational fluid dynamics (CFDs) simulations or other computational methods to model and simulate the combustion process. CFD simulations can provide detailed information on the flow dynamics, temperature profiles, and species concentrations within a combustion system, allowing for the investigation of complex combustion phenomena, such as flame propagation, ignition, and pollutant formation. (During hydrogen combustion, such as in a turbine used for electricity generation or in industrial heating applications, certain nitrogen oxides (NOx) can be released. Nitrogen oxides (NOx) production arises from the exposure of air, which consists of nitrogen and oxygen, to extremely high temperatures above 1500 °C). Computational investigations can provide insights into the fundamental processes and mechanisms governing hydrogen combustion, as well as optimize the combustion processes for efficiency and emissions reduction [10–12].

An Overview of the Importance of Combustion Processes

Converting fuel to combustion products is intrinsically complex due to the physical and chemical phenomena taking place during the process such as flame propagation, explosions, and fuel–oxidizer mixing. It is important to consider that not all fuel–air mixtures ignite or burn as there are certain limits of composition. This phenomenon is defined by the lower and upper flammability limits in which the mixture can burn. It is dependent on several factors such as pressure and temperature [4].

Studying the combustion processes that are employed to optimize the design, evaluate the burner's performance, and predict factors such as the flame temperature, emissions, and heat transfer characteristics is important. Additionally, combustion science can contribute valuable knowledge and methods for emission-related questions, combustion chemistry and diagnostics, and the physicochemical analysis, characterization, and monitoring of combustion-generated pollutants and aerosols. By taking chemical knowledge into account, combustion systems can be described, tailored, and improved [5]. The most important factors addressed in the study of combustion processes are the following: flame propagation, burning velocity, stability limits, flame dynamics, flame stretching, flame quenching, thermal energy generated, and emissions.

Theoretical investigations of hydrogen combustion involve the development of combustion models and mechanisms based on the fundamental principles of chemistry and physics. These models may be used to predict combustion behavior, reaction rates, and pollutant formation under various conditions. They can also provide insights into the molecular-level processes and mechanisms that govern hydrogen combustion, such as chemical reactions, reaction intermediates, and reaction pathways. Investigations of hydrogen combustion have a significant impact on expanding our knowledge of how hydrogen burns as a fuel, and in developing efficient and clean combustion technologies for hydrogen-based energy systems. This review discusses the advantages and considerations associated with combining pre-mixed combustion systems with hydrogen fuel, highlighting the potential of this approach to address environmental and energy challenges, to achieve the safe and sustainable use of hydrogen as an alternative energy source with potential applications in various sectors, including transportation, power generation, and industrial processes.

2. Observations on Burning Hydrogen in Premixed Combustion Systems

The following section provides an overview of the diverse range of research activities conducted on hydrogen-assisted gas fuel combustion. Properties such as the limitations of hydrogen-enriched hydrocarbons' flammability and the effects of adding hydrogen on ignition characteristics are discussed. The effect of the hydrogen addition on the flame front instability and laminar burning velocity of the hydrogen–hydrocarbon/air mixture and the effect of the addition of hydrogen on the lean premixed combustion emission and stability are reviewed.

2.1. Hydrogen Combustion in Burners

The equivalence ratio (ϕ) is a crucial concept in combustion science and engineering that measures the ratio of the actual fuel-to-air ratio to the stoichiometric fuel-to-air ratio. A more detailed representation is as follows: Fuel-to-Air ratio (actual)/Fuel-to-Air ratio (stoichiometric). Table 1 shows the equivalence ratio cases and their importance in combustion.

Table 1. The equivalence ratio cases and their importance in combustion.

Equivalence Ratio Cases	Importance in Combustion
▪ When $\phi = 1$, the fuel-to-air ratio is exactly stoichiometric. This is the ideal condition where there is just enough air to completely burn all the fuel. ▪ When $\phi > 1$, the mixture is rich in fuel (more fuel than stoichiometric, less air), which can lead to incomplete combustion and increased emissions. ▪ When $\phi < 1$, the mixture is lean (more air than stoichiometric, less fuel), which generally leads to more complete combustion but may result in higher temperatures and potentially higher NOx emissions. ▪ While the hydrogen-doping ratio means the percentage of enrichment hydrogen in gas fuel.	▪ Combustion Efficiency: The equivalence ratio helps in optimizing the combustion process. At $\phi = 1$, combustion is most efficient in terms of fuel usage. Deviations from this ratio can affect the efficiency and emissions of the combustion process. ▪ Emissions Control: Rich mixtures ($\phi > 1$) can produce more unburned hydrocarbons and carbon monoxide, while lean mixtures ($\phi < 1$) can produce more nitrogen oxides (NOx). Understanding and controlling the equivalence ratio helps in managing emissions. ▪ Engine Performance: In internal combustion engines, adjusting the equivalence ratio affects the power output and engine performance. Engines often operate at different equivalence ratios depending on the operating conditions (e.g., idle, full load).

Tang et al. [13] provided a thorough analysis of the recent developments in the major aspects of combustion enhanced by hydrogen. The investigation covered a wide range of subjects, including the lowest energy required for mixes of hydrogen and hydrocarbons to ignite and the ignition behavior of hydrogen/hydrocarbon fuel blends. The results showed that significant decreases in the energy required coincided with a higher portion of hydrogen and three distinct behaviors occurred with an increase in the hydrogen fraction. Furthermore, the hydrogen addition affected the flame-front instability behavior through a

combination of body force, the hydrodynamic effect, and the thermal-diffusion effect. A coaxial nozzle burner (CNB) was used to investigate the properties of the hydrothermal combustion of hydrogen by building a computer model of fluid dynamics and comparing it with the experimental data. Hydrothermal combustion is a rapid exothermic oxidation reaction that occurs in water above critical limits, which can be used in the treatment of highly concentrated organic materials. The flow field, the flame stabilization process, and the impact of various operating parameters on combustion in the CNB are then all simulated by this model. The results showed that, downstream of the injector, a V-shaped zone where reactants flow backward due to recirculation enhances the turbulence and heat transmission, which is where most combustion occurs. The combustion zone moved closer to the nozzle exit when the flame's length and width were reduced by gravity acting in the same direction as the jet. The kinetic rate and peak temperature can be enhanced by raising the feed temperature and concentration. By changing the reactant's residence period, the feed flow rate mostly modifies the axial temperature gradient close to the nozzle outlet.

The output of energy and performance of the integrated system of the combustor and photovoltaic generators are restricted by a short residence time, a high heat loss ratio, and flame instability [7]. To improve the generator's thermal performance and broaden its applications, this study used a combustor with an exit step to perform hydrogen–air premixed combustion at different CO mixing percentages. This study discussed multiple factors related to burner design and operation. The results showed the addition of carbon monoxide to hydrogen–air premixed combustion helped relocate and stretch the flame, resulting in a significant improvement in the comprehensive thermal performance of the burner. Additionally, the combustor structure enhanced the heat transfer and flame anchoring in an efficient manner. A suitable exit step height and length allowed for an increased radiation power. The stagger step further increased the radiation power and system efficiency [14]. A grey relationship analysis showed that the step height and CO fraction were important factors in radiation power and efficiency. Furthermore, the results demonstrated a high level of overall operational performance represented by a significantly increased radiation efficiency estimated at 24.8% compared to combustion in a straight channel flame, as shown in Figure 1. Generally, the micro thermo-photovoltaic generator (micro-TPV) is a system that uses hydrogen as fuel and is capable of delivering power on the order of a watt in a package less than 1 cm^3 in size. The results showed a maximum system efficiency at 2.62% and an electrical power of 2.33 W for this generator under a CO blended proportion of 15% and an equivalence ratio of 1.0. Chen et al. [15] confirmed that ammonia's high hydrogen density and carbon-free properties have led to increased interest in porous media burners fueled by ammonia for small to medium combustion and power equipment, as shown in Figure 2. This study explored the impact of pure ammonia combustion and hydrogen addition on ammonia combustion in a porous burner, using numerical simulations and experiments to facilitate the practical applications of ammonia as a fuel. The analysis assessed the influence of the porous burner parameters, hydrogen addition ratio, and equivalence ratio on ammonia's flame properties, temperature distribution, and conversation rate formation characteristics, as shown in Figure 2.

While Dai et al. [16] developed a numerical model with a double-layer structure and multi-step kinetic mechanisms to investigate the effect of the hydrogen injection position and width on methane combustion characteristics, following experimental validation. The results showed that axial temperatures during a hydrogen injection at the upstream and interface positions were significantly higher compared to the downstream position. As the hydrogen injection increased, the overall temperature gradually decreased, correlating with a reduction in CO and NOx emissions. However, as the equivalence ratio of methane and hydrogen increased, both the temperature and pollutant emissions also increased. Additionally, increasing the velocity of methane and hydrogen led to a higher CO emission and a lower NOx emission.

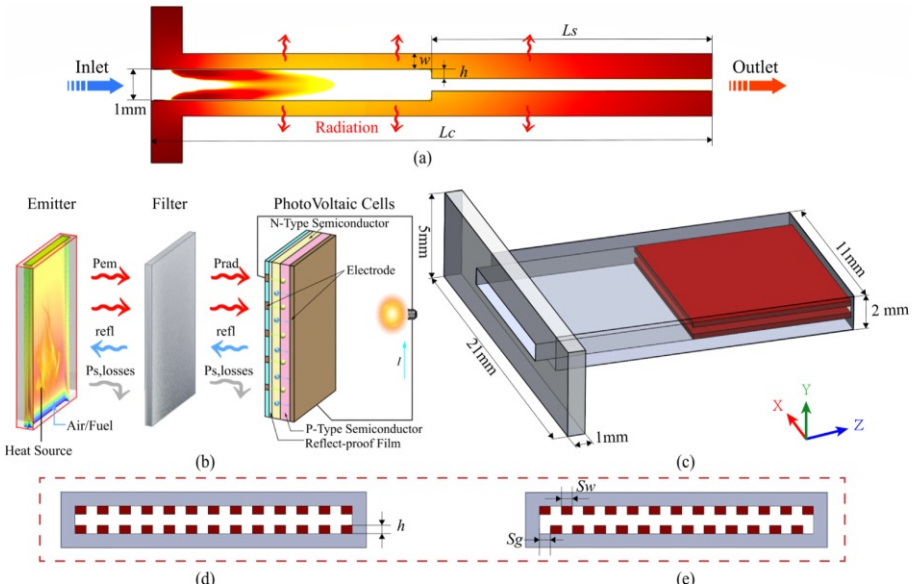

Figure 1. (**a**) Side view of burner, (**b**) diagram of a typical micro-TPV system, and the combustor with (**c**) exit step, (**d**) symmetrical gaps, and (**e**) stagger gaps [14].

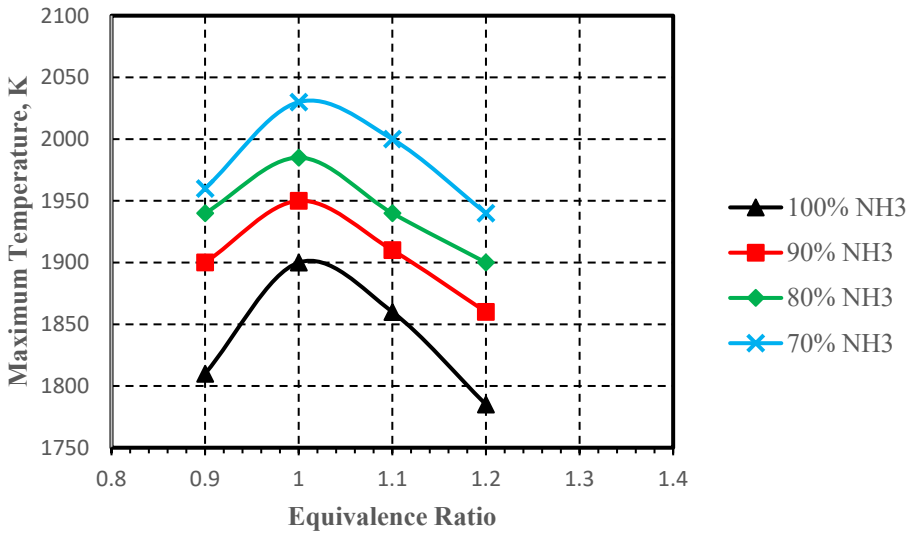

Figure 2. Maximum temperature with different equivalence ratios and hydrogen additions ratios [15].

Zhang et al. [17] conducted a numerical analysis to investigate the influence of hydrogen concentration on various aspects of methane–hydrogen–air flames. These aspects include the laminar burning velocity, flame stability (Markstein number), and flame temperature. The analysis covered a range of global equivalency ratios, specifically 0.7, 1.0, and 1.2. This investigation relied on comprehensive chemistry and the detailed transport of molecular species. The effects of the flame curvature were determined by studying the tubular flames and comparing them to the opposed-flow planar flames, while the effect of expansion rate on the combustion parameters was investigated using an opposed-flow planar flame model [17]. Also, the varying responses of the planar and curved flames to the hydrogen fraction were observed. The results demonstrate that as the hydrogen fraction increases, the flame temperature and laminar burning velocity also increase, with a more significant effect at higher stretch rates, and the Markstein length gets shorter in the interim. The Markstein number, named after the scientist George Markstein, is a dimensionless quantity used in combustion theory, particularly in the study of flame propagation and stability. Many researchers used it to analysis the effects of flame stretch, which refers

to the influence of the flame curvature and flow strain on flame speed and stability. The temperature of the tubular flame is significantly higher than that of the planar opposed-flow flame at a fixed stretch rate of 400/s, close to the extinction limit. On the other hand, the Dam Kohler number is used to characterize the relative significance of the reaction kinetics compared to the transport processes in a system. It can be particularly useful in scenarios involving chemical reactions and fluid flow, such as in reactors or during the dispersion of the substances in a fluid. Then, the discrepancy can be attributed to the influence of the positive flame curvature on the initial Dam Kohler number.

Liu et al. [18] studied in detail the effects of hydrogen additions on pipeline energy coefficients and the layout of pressurization stations. They also investigated the case of intermediate gas injection and examined the effects of injection positions. This research provides valuable insights for designing hydrogen–natural gas (H_2-NG) pipeline systems. The study revealed that as the hydrogen fraction increases, the distance between pressure stations also increases. Furthermore, overpressure happens if the original pressure station layout is kept. The input pressure for the pressurization stations that come after is lowered as a result of the intermediate gas injection. Therefore, when using existing pipeline networks to transport H_2-NG, it is essential to make the appropriate adjustments. Mayrhofer et al. [19] investigated the utilization of natural gas–hydrogen blends as a substitute for conventional fuel for commercial heat treatment furnaces and evaluated the financial viability of doing so in order to cut carbon dioxide emissions. An in-depth technological examination of the different factors affecting s heating system was conducted, along with an evaluation of the furnace heating technology challenges. The main thermos-physical characteristics of the mixtures and their corresponding flue gases were assessed to identify the heating system requirements, and potential methods for increasing heat transfer and decreasing flue gas losses were presented. An increase in the overall combustion efficiency of around 1.2% was seen in the radiant tube application when the fuel gas contained 40% hydrogen. The study also considered the influence of the air-to-gas ratio control system on the furnace. The ability of two widely used control systems to adjust the flow gas rate for blends with different hydrogen concentrations and combustion characteristics, such as the Wobbe Index, was evaluated. Demonstrating the feasibility of retrofitting existing furnaces is crucial. Different natural gas–hydrogen mixtures were used to evaluate two different burner types: an open jet burner with flameless and air-staged combustion operation modes and a recuperative burner for use with radiant tubes. Both systems' nitrogen oxide generation was assessed with varying fuel blends and operating circumstances. Compared to pure natural gas fire, a 40% hydrogen component resulted in a 100% increase in flameless combustion and a 10% increase in air-staged combustion.

Ozturk et al. [20] offered a cutting-edge integrated solution for combining natural gas and hydrogen for a specific home use. With the current configuration, an alkaline water electrolyzer unit produces hydrogen using electricity sourced from renewable sources like wind turbines and solar PV panels. The building where the system is installed gets any leftover electricity. The Engineering Equation Solver 4.0 (EES) and Aspen Plus 21 software are used to evaluate the system as a whole. In the blend, the volume fraction of natural gas is reduced from 100% to 80%, while the hydrogen portion is increased by volume from 0% to 20%. The combustion unit's carbon dioxide emissions decrease as the hydrogen input rises. The performance assessment indicates that the energy and energy efficiencies in March were the highest at 67.3% and 53.2%, respectively, while the lowest values were recorded in December at 58.4% and 44.2%, respectively.

Miao et al. [21] examined the effects of adding hydrogen (H_2) on pollutant emissions from an inverse diffusion flame (IDF) that burns liquefied petroleum gas (LPG). The study focused on the emission behavior of pollutants in fuel-lean conditions, measuring the carbon oxides (CO, CO_2, and HC) and oxides of nitrogen (NOx) coming from the flame and reporting their emission indices. Both CO and HC emissions are strongly influenced by the overall equivalence ratio, with high levels at fuel-lean conditions and levels decreasing to almost zero at equivalence ratios above 0.8 in LPG-H_2 IDF. NOx emissions follow the

HC trend due to the N_2O-intermediate and Fenimore mechanisms in fuel-lean conditions, while increasing with the equivalence ratio in fuel-rich conditions because of the thermal NOx mechanism. Hydrogen addition has been observed to enhance the conversion of CO and HC into CO_2. A threshold hydrogen fraction exists, beyond which there is a substantial reduction in CO and HC emissions. A high air jet Reynolds number can lead to an inefficient combustion, resulting in increased HC, CO, and NOx emissions. In comparison to LPG IDF, LPG-H_2 IDF starts generating noticeable CO and HC emissions earlier, with both the CO and HC emissions being more significant.

Han et al. [22] highlighted the uncertainty in the laminar burning velocity (LBV) measured by several organizations and the approach used was the outwards spreading spherical flame technique, which involves studying the combustion of hydrogen–air and syngas–air mixtures under normal temperature and pressure conditions, and identified the underlying reasons of uncertainty. As illustrated in Figure 3, it was discovered that the (LBV) measurements exhibit significant variability, making these empirical data untrustworthy for reducing the level of uncertainty in chemical models. The sources of uncertainty are examined in various flame propagation regimes, and 1-D simulations are used to evaluate each source's contribution to the disparities. The findings indicate that ignition effects may be one of the primary causes of error for the laminar burning velocities of fuel-rich mixes, and that their contribution to uncertainty is highly dependent on the equivalency ratio. Moreover, the selection of the extrapolation model and the range of flame radius has a considerable impact on the accuracy of the laminar burning velocities that are observed. Nonlinear extrapolation is more robust to variations in the flame radius range than linear extrapolation. It is possible to lessen the effect of the chosen flame radius range on uncertainty when employing nonlinear extrapolation models, particularly for combinations that are fuel-rich or fuel-lean. However, strong nonlinear behavior between the stretched flame speed and the stretch rate still contributes to large discrepancies even when nonlinear extrapolation models are used. To address the nonlinear stretch behavior, a new nonlinear extrapolation model, NQH, is proposed and is shown to be more accurate than other models as pressure increases. Additionally, recommendations for the H_2 and syngas LFS measurements using the OPF method are provided.

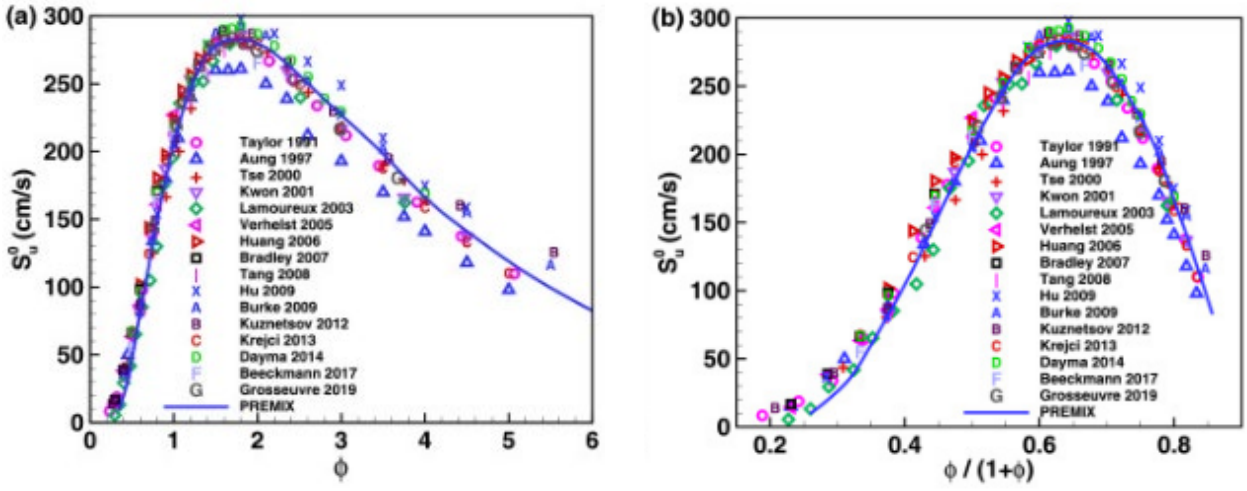

Figure 3. Laminar burning velocity (vertical axes) of H_2/air at NTP as an expression of the equivalence ratio (horizontal axes) (**a**). Standard equivalence ratio (**b**). The symbols represent empirical findings from multiple investigations [22].

Ilbas et al. [23] measured the laminar burning velocities of hydrogen in air and varied mixes of hydrogen and methane in air (from 100% methane to 100% hydrogen), which were recorded at room temperature for a range of equivalency ratios (ER = 0.8–3.2). For this experimental inquiry, a modified test rig based on the former 'Cloud Chamber' at

Cardiff University was created. The apparatus comprises a cylindrical explosive bomb made of stainless steel, measuring 250 mm in length. At one end, a stainless-steel plug is enclosed to house an internal stirrer for mixing purposes. A round quartz window with a 120 mm diameter seals the other end. Two diametrically opposed quartz windows on both sides provide optical access for filming the flame propagation. High-speed Schlieren photography was used to determine the flame speeds within the bomb. The burning velocities were subsequently determined using a CHEMKIN computer model (US company, Albuquerque, NM, USA) to compute the expansion ratio. The test facility's design ensures a laminar, spherical flame unaffected by buoyancy. The empirical findings demonstrated that augmenting the proportion of hydrogen in the hydrogen–methane amalgamation resulted in an elevation in the rate at which combustion occurred and an enlargement of the range within which the combination was capable of igniting. The experiments also suggested that a hydrogen–methane blend (e.g., 30% hydrogen and 70% methane) could be a competitive alternative fuel for existing combustion plants. Ma et al. [24] carried out a number of tests using methane–hydrogen–air mixes in a 20 L spherical explosion vessel at beginning conditions of 1 atm and 293 K. The fuels' hydrogen content varied from 0% to 100%. Regardless of the fuel equivalency ratio, it was found that the peak temperature constantly trailed the peak pressure in arrival time. Because of heat loss, the experimental peak overpressure values were lower than the adiabatic ones. Additionally, it was discovered that adding hydrogen might, in experiments, raise the temperature and explosion pressure while marginally lowering both in adiabatic settings. There is a linear relationship between the amount of hydrogen and both the rise in experimental and the fall in adiabatic circumstances. Consequently, the difference between the adiabatic and experimental measurements decreases with the hydrogen proportion increases. Moreover, the positive effect of the hydrogen addition on the dp/dt max is minimal at low hydrogen proportions but becomes much more pronounced at higher hydrogen contents, exhibiting exponential growth. For each fuel composition throughout all the experiments, the peak overpressure, peak temperature, and dp/dt max for the fuel equivalence ratios of 0.6, 1, and 1.5 follow the same pattern: $\phi = 1$ is the highest, followed by $\phi = 1.5$, and $\phi = 0.6$, as shown in Figure 4. Finally, as a function of the hydrogen percentage, the lowest ignition energy of the gaseous methane–hydrogen–air mixtures at a fuel equivalency ratio of 1.5 was determined. It exhibited a steep decline from 118 MJ for methane–air to 0.12 MJ for hydrogen–air as the fuel's hydrogen content rose. Additionally, it was found that the linear weighted sum of the minimum ignition energies of each component, with the volume fraction of each component serving as the weighting factor, may be used to roughly compute the minimum ignition energy of multi-component gas mixtures. For a given multi-component gas, this can be thought of as a universal technique for figuring out the lowest ignition energy.

Miao et al. [25] discovered experimentally that the addition of hydrogen significantly increases the LPG's laminar burning velocity, with a more significant acceleration when the hydrogen content rises above 60%. At different equivalency ratios, the impact of the hydrogen addition on diffusion thermal instability as indicated by the Markstein length was examined. The addition of hydrogen results in a decrease in flame thickness; hydrogen has a less significant effect on flame thickness than the equivalency ratio. The flame thickness values for a fuel mixture of 10% LPG and 90% hydrogen are consistent for all the equivalency ratios, as shown in Figure 5. Sun et al. [26] examined laminar spherical flames propagating within a homogeneous hydrogen–air mixture, focusing on the effects of initial conditions such as the equivalence ratio, initial pressure, and initial temperature on the propagation characteristics. During propagation, the global stretch rate decreases steadily towards convergence. It initially increases and then decreases as the equivalence ratio (Φ) rises from 0.5 to 4.0, with the maximum value occurring at $\Phi = 1.8$. The propagation speed constantly climbs within stoichiometric and rich mixtures, but dips and then rises within lean mixtures when the global stretch rate decreases. The initial temperature does not affect the Markstein length, but the equivalency ratio and initial pressure do. While the variation of the starting thermodynamic circumstances changes the unstretched LBV

consistently, the variation of the equivalency ratio does not change it equally. The flame gets increasingly unstable as a result of the reduced stretch effects. Hydrodynamic and thermal-diffusive processes are used to look at the connection between the starting conditions and the critical flame radius of cellular behavior. Furthermore, the critical Peclet number is found to be linearly related to the equivalence ratio, but it is less sensitive to the initial ambient conditions.

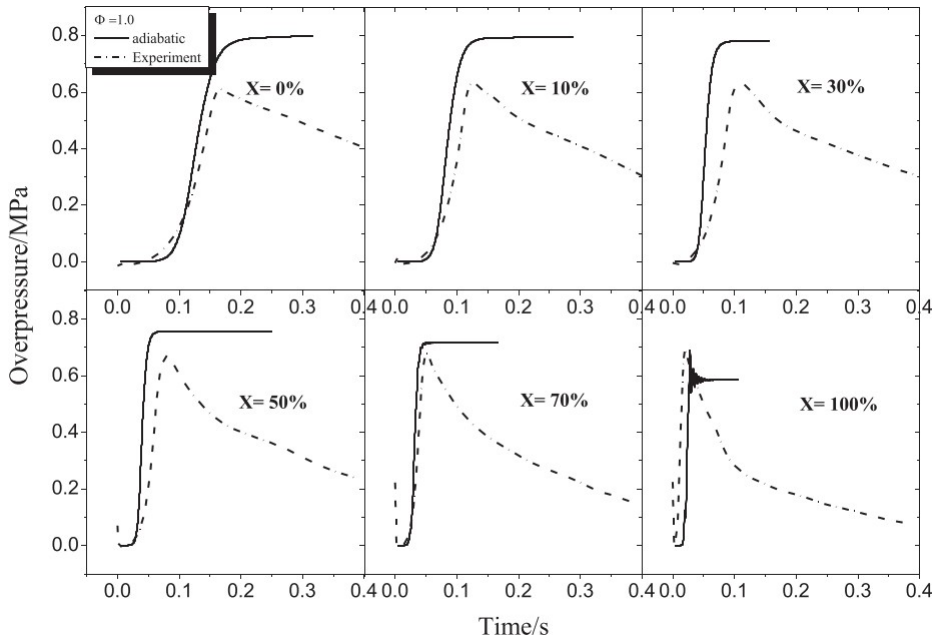

Figure 4. Comparison of the measured and calculated adiabatic overpressure histories of stoichiometric methane–hydrogen mixture [24].

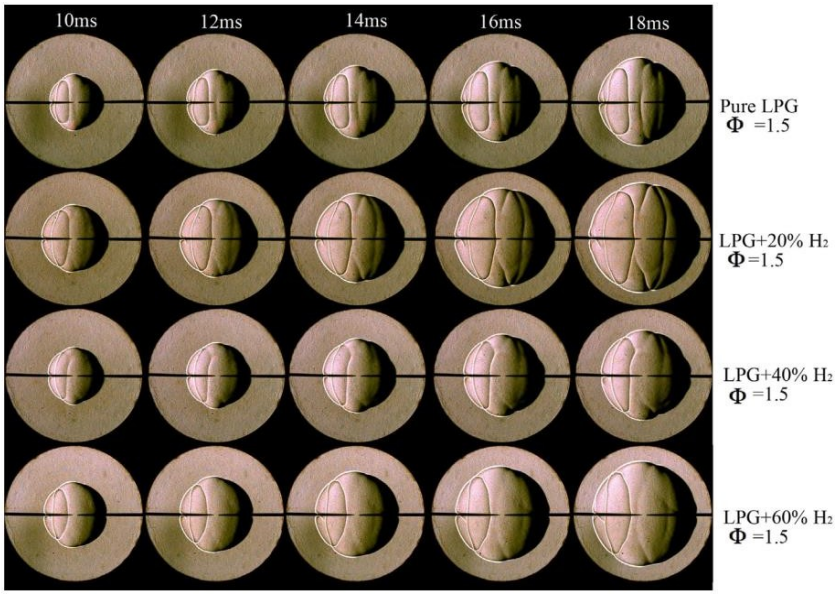

Figure 5. Schlieren photographs of LPG and LPG/Hydrogen mixture at 0.1 MPa, 300 K [25].

Liang et al. [27] have decided to use Frankel and Sivashinsky's finite flame thickness formula for extrapolation. By utilizing numerically generated stretched flame data from outwardly expanding spherical flames for lean and rich hydrogen–air and n-heptane/air mixtures, they show that the laminar flame thickness and Markstein length are simultaneously yielded by the finite thickness expression, improving the extraction of the laminar

flame speed. Furthermore, the causes of the errors in earlier linear and nonlinear extrapolation expressions, the impact of pressure on the extrapolation outcomes, and the resilience of different expressions in accommodating experimental errors were examined.

The effects of the blow-off of the lean premixed flames, the laminar flame speed on the onset of local extermination, and the density ratio, stabilized in a mesoscale bluff-body combustor, on the hydrogen–air and syngas–air mixtures were investigated using direct numerical simulations. To separate the two parametric influences on the flame time scale and fluid dynamic instability, six simulated situations were looked at by Kim et al. [28]. Under a variety of velocity settings, the flame progress approaching the blow-off limit in all cases followed a series of five distinct modes, with probable cyclic patterns among these modes. Both the vortex street modes and asymmetric vortex shedding were associated with the local extinction onset. The increasing sinuous mode, suitably scaled by the Strouhal number, intensifies flow instability as the density ratio drops. The competition between the duration of flow residence time linked to the lateral flame movement and the delay in the ignition of local mixtures determines the onset of local extinction and blow-off. Additionally, fluid dynamic influences also impact the velocity at which a blow-off occurs. The validity of the conclusions was supported by a time-scale analysis for all situations that were looked into [28].

Cardona et al. [29] scrutinized the combustion characteristics of a syngas blend, comprising hydrogen, carbon monoxide, and carbon dioxide, in the absence of a visible flame by utilizing heated and diluted streams. The studies were carried out utilizing a jet in a hot co-flow burner, which consists of a core fuel jet surrounded by a stream of combustion products, as depicted in Figure 6. The jet nozzle was used to release the syngas mixture, resulting in the attainment of a high temperature and low oxygen concentration in the jet flame [30–32]. Three distinct oxygen compositions of 2.0%, 4.7%, and 6.9% were examined in the oxidant stream. Measurements of the temperature and species concentration were taken along the axial and radial lines at a constant Reynolds's number. The results indicate that elevating the oxygen content leads to a decrease in the CO and NO emissions throughout the entire process. Mihaescu et al. [33] focused on the key factors involved in designing a hydrogen burner. Using Ansys-Fluent software 14.0, numerical modelling was employed to establish the relationship between the flow velocity of the combustible gas jets, the required air, and the combustion rates. Combustion models, both analytical and numerical, were used to determine the optimal ratios between the combustion and flow velocities, as well as how they compared to those used for methane combustion. These findings were then correlated with the established guidelines and recommendations for burner designs.

Vance et al. [34] investigated the behavior of pure hydrogen–air flames stabilized behind a cylindrical bluff body using experiments and numerical simulations. The results of the computational fluid dynamics simulations are validated qualitatively against the experimental data, and the role of stretch and preferential diffusion in the process is examined. It is important to note that, while there is currently no scaling reference for such flames, this study finds that the displacement speed of flames stabilized beyond the lean flammability limit of a flat stretch less flame (φ = 0.3) can be scaled with a suitable tubular flame displacement speed. Additionally, this study explains why excessive local stretching causes such flames to extinguish and validates the theory on the lean limit blow-off for flames with a neck structure. Within a recirculation zone, closed flame fronts stabilize following the extinction of the flame neck. These findings contribute to a better understanding of the underlying physics that governs the behavior of ultra-lean hydrogen flames, which can be used for designing safer and more efficient combustion devices. Mitu et al. [35] examined the impact of adding hydrogen on the LBV of methane–air and natural gas–air mixtures through experimental and numerical investigations, by using mixtures with equivalence ratios ranging from 0.90 to 1.30 and hydrogen fractions (r_H) varying between 0.0 and 0.5. Under ambient starting circumstances, the experiments were carried out in a 14 L spherical tank equipped with a central ignition. Only the early stage of flame propagation—which

was estimated using p (t) data in compliance with EN 15967 [35]—was used to calculate the LBVs. The findings show that the addition of hydrogen causes the LBV of every binary flammable mixture under investigation to rise. The variation of LBV with respect to r_H follows a linear trend at moderate hydrogen fractions but becomes more significant with further increases in r_H, as shown by both the experimental and computed LBVs. The addition of hydrogen also significantly alters the thermal diffusivity of flammable CH4–air or NG–air mixtures, the rate of heat release, and the concentration of active radical species in the flame front, all of which contribute to LBV variations. These findings provide insight into the effects of a hydrogen addition on the combustion characteristics of methane and natural gas mixtures, which have implications for optimizing combustion efficiency in practical applications, as shown in Figure 7. Raman [36] studied hydrogen concentrations below 10%, an area with limited data due to the previously mentioned challenges. These extremely lean hydrogen–air flames are of particular interest due to their unusual behavior near the lean limit. The current kinetic models for hydrogen–air combustion are effective near stoichiometric conditions but fail in the extremely lean regime.

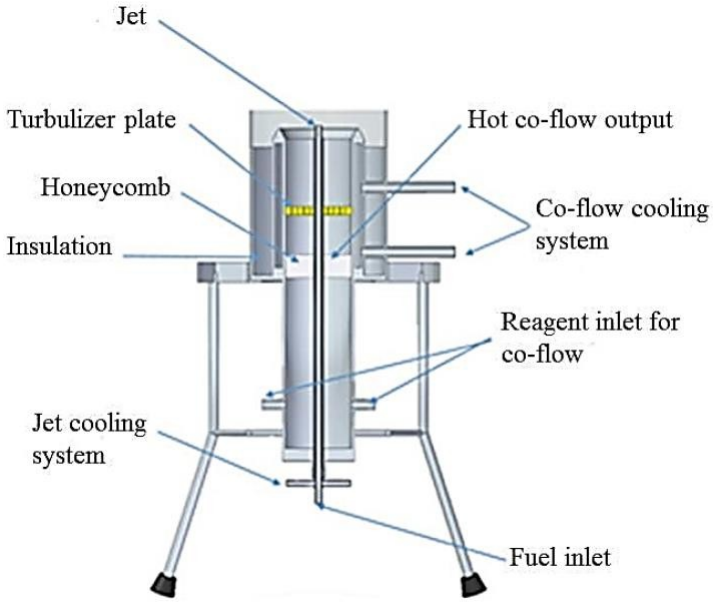

Figure 6. A jet in hot flow burner scheme [29].

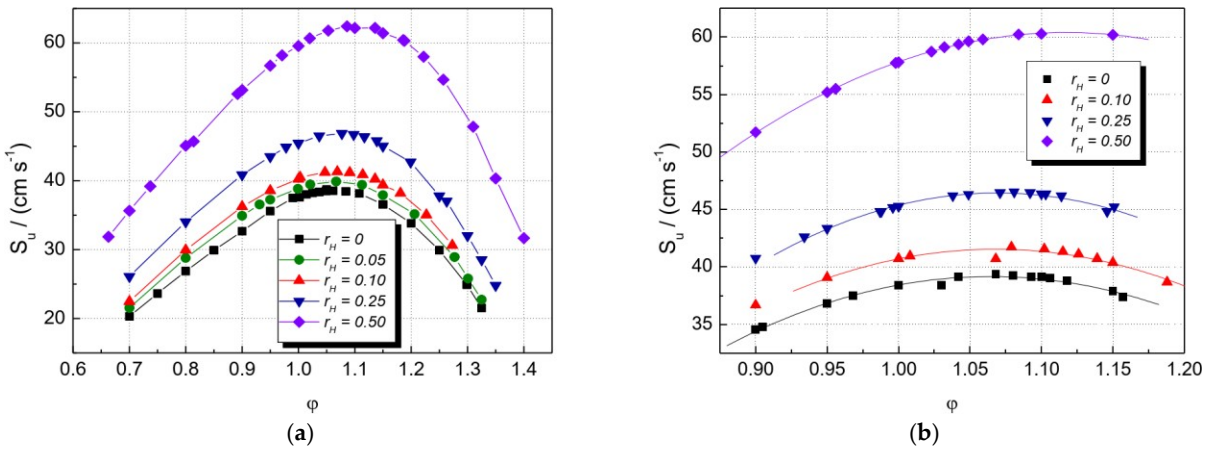

Figure 7. Computed laminar burning velocities of single fuel–air and multifuel–air mixtures with various fraction of hydrogen at ambient pressure and temperature (**a**) CH_4–H_2–air, and (**b**) NG–H_2–air mixtures [36].

This could be attributed to a fundamental shift in the combustion mechanism, as different elementary reactions become crucial at the low temperatures associated with lean hydrogen combustion [36]. The combustion temperatures in lean hydrogen–air flames are significantly less than those observed with other fuels, as hydrogen's high diffusivity relative to air allows it to burn at leaner concentrations. In order to understand and explain this peculiar behavior, reliable experimental data on the lean combustion characteristics of hydrogen are essential for both motivating and validating the theoretical models. The primary objective of their study was to establish dependable experimental data for the laminar burning velocities of extremely lean hydrogen–air mixtures [36]. Ren et al. [37] investigated the impact of adding hydrogen on the combustion characteristics of natural gas. Detailed chemical reaction processes were employed with the ChemKin II/Premix Code, ensuring that the sort effect was taken into account in every computation. The hydrogen mole fraction in the fuel can be changed from 0 to 40% at various beginning pressures (1–8 atm) and temperatures (298–500 K) to determine the adiabatic flame temperatures and laminar burning velocities of C1–C4 alkanes, which were found to increase with the increasing hydrogen-doping ratio. (The hydrogen-doping ratio typically refers to the proportion of hydrogen atoms introduced into a material (like semiconductors, metals, or other compounds) to modify its properties. This ratio is crucial in various applications, such as improving electrical conductivity, enhancing catalytic activity, or adjusting optical properties).

Methane showed the highest increase in laminar burning velocities and the adiabatic flame temperature increased with the hydrogen-doping ratio. The production of active radicals (H, O, and OH) during combustion was strongly correlated with the laminar burning velocities. The sensitivity of the flame temperature in the four alkane fuels present in the natural gas was analyzed at the maximum temperature gradient. At a constant hydrogen-doping ratio, increasing the initial temperature significantly increased the laminar burning velocities and adiabatic flame temperature. With increasing pressure, the laminar burning velocities gradually decreased while the adiabatic flame temperature increased. Table 2 presents the information of the design properties of the combustors used by different research groups, including the following: the range of equivalence ratios for the hydrogen–air mixtures, the initial conditions, and the flame analysis technique.

Table 2. Summary of experimental studies on laminar burning velocity measurements of hydrogen–air mixtures.

Authors	Range of Equivalence Ratios for H_2/Air Mixtures	Initial Conditions	Flame Analysis Technique	Remarks
Chen [15]	0.9–1.3	Ambient conditions	Absorbing column and gas analyzer	Effect of hydrogen addition on ammonia combustion.
Miao [21]	0.3–1.4	Liquefied petroleum gas with gradual hydrogen addition	Inverse diffusion flame burning	Hydrogen is promoted with the conversion of CO and HC to CO_2.
Ilbas [23]	0.8–3.2	From 100% methane to 100% hydrogen	High-speed Schlieren photographic technique	70% methane + 30% hydrogen could be a competitive alternative fuel for existing combustion plants.
Sun [26]	0.5–1.8	Pressure (1–5) bar Temperature (300–450) K	Schlieren system and high-speed camera	The unstretched laminar burning velocity does not exhibit a consistent change with variations in the equivalency ratio. However, it does consistently correlate with variations in the starting thermodynamic condition.

Table 2. *Cont.*

Authors	Range of Equivalence Ratios for H_2/Air Mixtures	Initial Conditions	Flame Analysis Technique	Remarks
Mitu [35]	0.9–1.3 with various hydrogen fractions 0.0–0.5	Ambient inlet conditions	Partial pressure method with total pressure (2–5) bar. COSILAB software 3.3	Increasing the fraction of hydrogen has an effect on the increase in laminar burning velocity.
Ren [37]	0.7–1.3 With mole fraction of hydrogen varying from 0–40%	Pressure (1–8) bar Temperature (298–500) K	Numerical models GRI 3.0 USC Mec 2.0 San Diego	At a constant hydrogen-doping ratio, the temperature of the adiabatic flame rose noticeably as the inlet temperature rose.

2.2. Hydrogen Combustion in Micro Combustors

As a result of the need for hydrocarbon fuel energy as the most efficient in industrial applications, the research to develop miniaturized systems supported by high-quality energy devices has directed the interest of combustion applications towards micro-scale technologies [38,39]. One of the most important examples of this is the miniaturized liquid-fueled combustion device that is widely used as a highly efficient power supply compared to the most powerful batteries currently available.

Wei et al. [38] investigated the use of a block and no block in a micro heat-recirculation combustor for the combustion of premixed H_2/air. Additionally, the impact of the flow rate, heat recirculation, and block configuration on the combustion parameters and thermal performance were investigated. The block reduced heat loss through exhaust gas and increased flame stability and preheating, according to the data. But it also reduced the residence period of the reactants. A transverse block setting provided better thermal performance than a longitudinal one, with an increase in block height resulting in a broader high-temperature zone and improved radiation. On the other hand, a 10 mm tall block reduced the heat recirculation's effects and lowered the temperature of the outside wall. Proper placement of the block and block height can greatly enhance radiant efficiency, heat transfer, and micro power generator optimization. In Tan et al. [39], a three-dimensional mathematical model was built to achieve a homogeneous and elevated wall temperature distribution in micro combustors with rearward-step structures, using premixed hydrogen–air mixtures. It looked at how the inlet velocity and rearward-step architecture affected the micro combustor's thermal performance and combustion characteristics. The micro combustor's flame stabilization and combustion intensity were both enhanced by the rearward-step structure, according to the results. As demonstrated in Figures 8 and 9, an increase in rearward-steps from one to three produced an improvement in the lower and higher flammability limits of 20% and 3.5%, respectively, and a maximum combustion efficiency difference of roughly 2.28% at an input velocity of 7.0 m/s. Nevertheless, in the micro combustor, the rearward-step construction raised the mean outside wall temperature and worsened the outer wall temperature uniformity. The combustor with three stages had a mean outer wall temperature and temperature differential that were 6.3 K and 39.6 K higher, respectively, than the combustor with one step at an intake velocity of 5.0 m/s. In the micro combustor with three phases, the maximum synergy degree was 2.99% with an equivalency ratio of 1.5 and an inlet velocity of 7.0 m/s.

Peng et al. [40], using both experimental and numerical methods, examined the thermal performance and combustion properties of premixed hydrogen/propane/air in a micro planar combustor with a block insert. The impacts of the block width, flow velocity, equivalency ratio, and hydrogen blended fraction on heat transfer and flame stability were examined in the results. The findings showed that adding hydrogen to the micro combustor increased its combustion stability, with the lowest hydrogen blending mole percentage discovered via research using experiments, as depicted in Figure 10. A high fuel rate

block (0.7 mm) put into the combustor produced the largest range of combustion stability. Additionally, the block size and hydrogen blending ratio had a substantial impact on the wall temperature; a greater radiation temperature was obtained with an acceptable block width and H_2/C_3H_8 mixed burning temperature. The effects of the hydrogen fraction on reaction pathways were also examined in the study. The rates of OH and H production were determined by evaluating the reactions of $H + O_2 = OH + O$ and $H_2 = OH + H$, which revealed significant effects on the reaction area and flame location. It was discovered that, for the same chemical energy input of Ec = 90.6 W, the combustor, designated as C0.7, which was fueled with 90% hydrogen, attained the maximum average wall temperature of 1150.3 K and a radiation power output of 27.9 W.

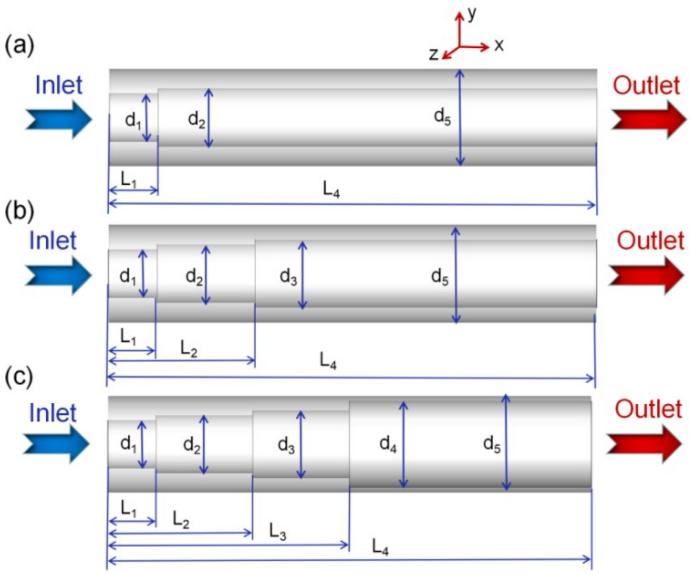

Figure 8. Geometries of the micro combustors (**a**) combustor with 1 step, (**b**) combustor with 2 steps, and (**c**) combustor with 3 steps [39].

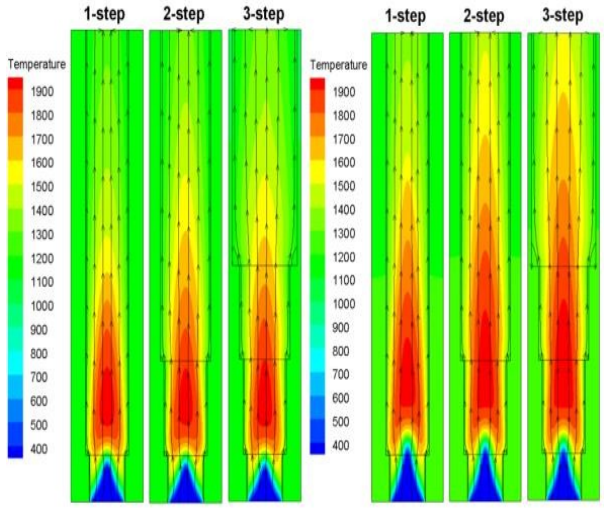

Figure 9. The flow field's streamlines and the gas temperature distribution at the XY plane can be visualized using a 2-step process [39].

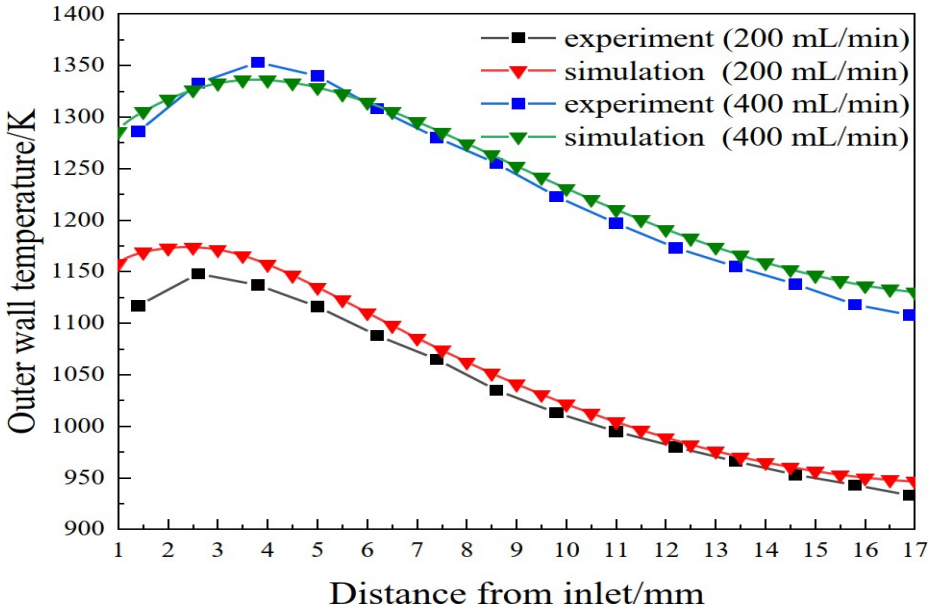

Figure 10. Comparison of the numerical data with the experimental result at 90% hydrogen addition and an equivalence ratio of 0.8 in the combustor [40].

Shi et al. [41] investigated premixed hydrogen and air combustion in a micro combustor featuring dual inlets. The study examined the influence of second-inlet configurations on combustion properties, thermal efficiency, and radiative performance. The findings reveal that adjusting the second inlet effectively alters combustion behavior and heat transfer, leading to an enhanced thermal performance in the burner. As the distance between the two inlets increases, the mean outer wall temperature initially rises and then falls, with a constant reactant ratio at the second inlet. This modification also impacts the flow field and radiative temperature. Yilmaz et al. [42] adopted a colorless distributed combustion technique for reduced pollutant emissions during the combustion of fuel and oxidizer mixtures. This work utilized numerical simulations to examine the properties of hydrogen and air mixes in a micro combustor. The objective was to tackle the difficulties associated with micro combustion and attain a more consistent temperature distribution along the outside wall. In order to investigate the potential of a colorless, dispersed combustion technique, the ANSYS/Fluent CFD system was used to simulate the combustion of hydrogen and air. The simulation was conducted at a constant equivalency ratio of 1.0, a heat input of 100 W, and varying mixture inlet temperatures of 300 K, 600 K, and 1000 K. Researchers attempted to achieve colorless distributed combustion technique conditions by reducing the oxygen concentration from 21% to 9% in 3% increments. The results demonstrated that colorless dispersed combustion conditions could be achieved at different oxygen concentrations, irrespective of the initial temperature of the mixture. However, at 300 and 600 K, these conditions did not positively affect the micro combustor's power output. In contrast, at 1000 K and an oxygen concentration of 9%, all combustion and emission performance metrics improved, potentially increasing the power output of the micro power generator.

In one of the power generators, the micro power system consisted of a compressor, combustor, turbine, and electric generator. Although they run on fossil fuels as diesel generators do, they have the advantage of being easily modified to recapture waste heat, making them ideal for cogeneration. Micro turbines are subject to minimum and maximum power rating constraints, similar to diesel generators. Barati et al. [43] created an analytical model to replicate the energy efficiency of a Micro Gas Turbine (MGT) powered by mixes of Hydrogen Enriched Natural Gas (H_2NG). The simulation results were validated using an experimental campaign conducted under the actual operating conditions of the MGT. The experimental effort for model validation occurred throughout the spring and summer seasons. Furthermore, the performance of the MGT was evaluated using H_2NG fuel

with hydrogen concentrations ranging from 0% to 10% by volume, with increments of 2%, as depicted in Figures 11 and 12. Based on the primary results, fuel consumption had a notable decrease, while heat recovery and electrical dependability showed minor enhancements, despite being influenced by environmental circumstances. A MATLAB R2020b–Simulink numerical model was constructed to accurately replicate the operation of the MGT. Therefore, the relative standard errors impacting the main output parameters were calculated.

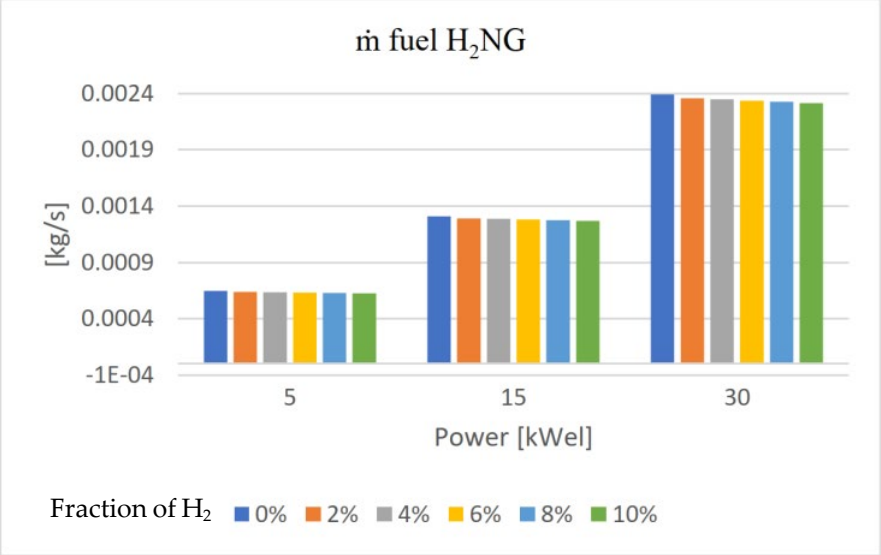

Figure 11. Divergence mass of fuel flow rate with H_2% at 5, 15, and 30 k Wel [43].

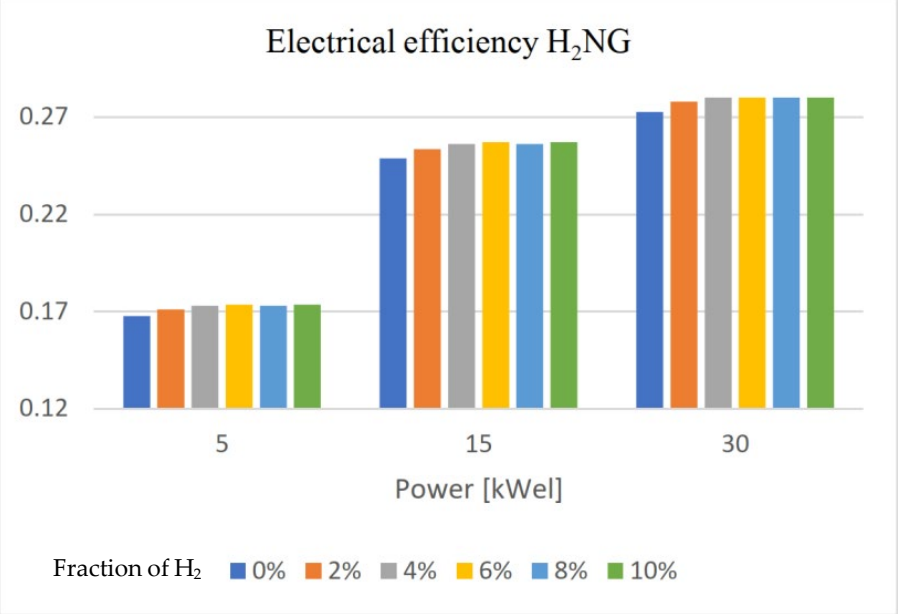

Figure 12. Divergence of electrical efficiency with H_2% at 5, 15, and 30 kWel [43].

3. Hydrogen as a Clean Energy Vector

3.1. Hydrogen's Potential as a Clean Energy Carrier

As stated in the UN Paris Agreement of 2016, achieving universal energy access and limiting the rise in the global temperature this century to well below 2 °C above the pre-industrial levels will require a significant decarbonization of large portions of the world's energy systems [44]. Hydrogen is considered a powerful catalyst for achieving a

low carbon future and has recently gained renewed attention as a clean and sustainable energy carrier to help achieve major reductions in emissions [45]. Sector coupling is facilitated by hydrogen in the world's energy networks and a profound emissions reduction is made possible in industries that are challenging to electrify in order to decarbonize [46]. Hydrogen enhances the incorporation of a higher proportion of variable renewable energy technologies (RETs) into the energy blend, while simultaneously enhancing the adaptability of a power system [47]. The technology is anticipated to have a vital function in equalizing the sporadic generation of solar and wind energy, as it has been identified as the most auspicious remedy for storing significant amounts of carbon-free energy over extended periods of time [48]. By harnessing electricity generated from renewable energy sources (such as Renewable Energy Technology) or other low carbon technologies, it is possible to make hydrogen with minimal or no carbon emissions through a process called water electrolysis. This hydrogen can then be stored using a method known as power-to-gas [49]. The stored hydrogen can then be used in a fuel cell system or burned in a gas turbine to generate energy as needed. As a result, hydrogen has a crucial role to play in lowering the power sector's reliance on fossil fuels and maintaining energy security. Dincer et al. [50] outlined a revolutionary method for utilizing Black Sea natural gas and hydrogen sulfide to efficiently develop an integrated fuel processing system that will speed up the shift to a hydrogen economy. The electrolyzer in the proposed system gets its electricity from offshore wind and offshore photovoltaic power facilities. Deep-water Black Sea hydrogen sulfide is converted to hydrogen via a proton exchange membrane electrolyzer unit. High-pressure tanks are used to store the hydrogen and sulfur gas produced for later use. Natural gas and hydrogen are combined and utilized in both commercial and residential settings. Aspen Plus software is used to model the system, and the processes of hydrogen production, blending, and combustion are studied in accordance with the model. The amount of hydrogen that can be added to the blend up to 20% reduces the annual cost of natural gas from USD 9 billion to USD 8.3 billion and reduces the carbon dioxide emissions from combustion from 14.7 ppm to 11.7 ppm. With a 20% by volume addition of hydrogen to natural gas, the energy and exergy efficiencies for the combustion process increase from 84% to 97% and from 62% to 72%, respectively. Olabi et al. [51] give a general review of the main technologies for producing and storing hydrogen, along with the difficulties they face. The goal is to find technologies that have enough promise for use in hydrogen-based large-scale energy applications. Hydrogen may be produced from water and fossil fuels and stored underground using the most efficient large-scale production and storage technologies. To enable significant large-scale hydrogen production and storage, however, a combination of solutions may be required, as regional variables play a crucial role in selecting the most appropriate methods of production and storage. Qazi et al. [52] summarized an overview of the latest advancements in hydrogen technologies across various sectors, including fuel refining, hydrocarbon processing, materials manufacturing, pharmaceuticals, aircraft construction, and electronics. The article summarizes the current industrialization scenario and explores prospective innovations, such as theoretical scientific advancements, green raw material production, potential exploration, and renewable resource integration. Additionally, the article discusses the socioeconomic implications of hydrogen as a green resource, as shown in Figure 13 [53].

Rosen et al. [54] discussed the role of hydrogen as an energy carrier, the technologies involved in hydrogen energy systems, and their economic aspects, as shown in Figure 14. Additionally, they examined the social and political implications of hydrogen energy, and addressed questions concerning when and where hydrogen is likely to gain significance. The key points are illustrated through relevant examples.

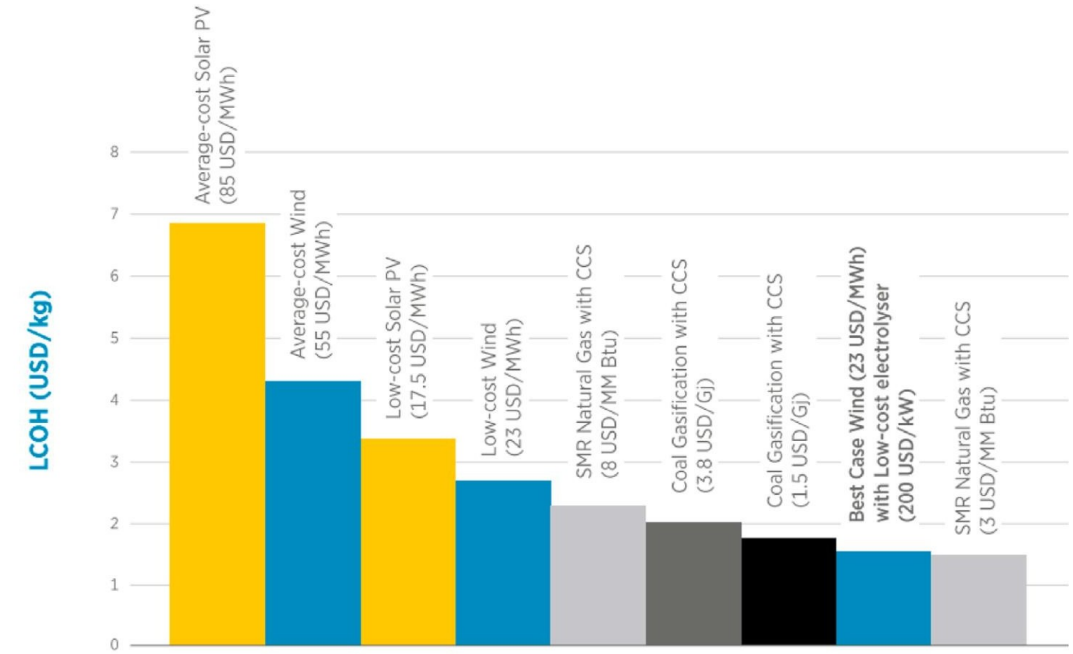

Figure 13. Hydrogen production cost for renewable and non-renewable energies in 2019 [53].

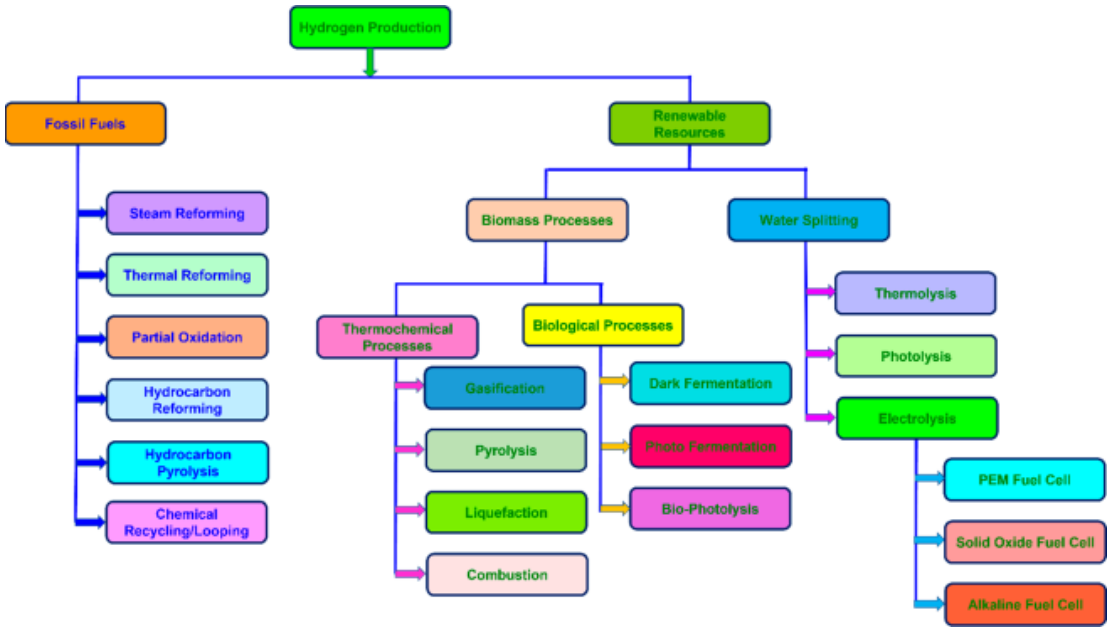

Figure 14. Hydrogen production technologies [54].

3.2. Hydrogen as Stimulating Fuel in Gas Turbines

In the quest for cleaner and more sustainable sources of energy, hydrogen has emerged as a promising candidate. With its high energy content, abundance, and versatility, hydrogen has gained attention as a potential solution for reducing greenhouse gas emissions and mitigating climate change. One area where hydrogen shows great potential is as a stimulating fuel in gas turbines, offering a pathway towards more efficient and environmentally friendly power. Hydrogen has several attributes that make it an attractive fuel

option for gas turbines. First and foremost, hydrogen has a high energy content, with three times more energy per unit weight than natural gas. This means that hydrogen can provide the same energy output with lower fuel consumption, reducing the amount of fuel needed and hence the greenhouse gas emissions associated with combustion. Benaissa et al. [55] utilized numerical investigations to examine the properties of combustion for a biogas fuel mixed with hydrogen in different ratios for a non-premixed whirling flame in a gas turbine combustor in the form of a can. The study considered hydrogen enrichment ranging from 0 to 50% by volume utilizing the non-premixed flamelet model, turbulence standard (k-ε) model, and P-1 radiation model to forecast the power of the can-type combustor at a constant operating power of 60 kW. The effects of the hydrogen enrichment, global equivalency ratios, and various swirl numbers on the temperature distribution and contours, velocity streamline contours, NO emissions, and species concentrations were also examined using the steady laminar flamelet model. The results showed that the hydrogen enrichment, equivalence ratio variation, and swirl numbers had significant impacts on the flame macrostructure. Hydrogen enrichment intensified the combustion, resulting in a higher flame temperature and wider flammability compared to pure biogas. For biogas and biogas–50% H_2, the maximum NO emissions in the output chamber dropped by 43 and 78 (ppm @15% by volume of O_2), respectively, as a result of a lower flame temperature that decreased the thermal NOx generation and lowered the equivalency ratio from 0.5 to 0.2. At the same equivalency ratio, pure biogas (0% H_2) and a high rate of hydrogen (50% H_2) showed an identical flame temperature and NO emissions at $\phi = 0.2$. CO and CO_2 emissions decreased with decreases in the equivalence ratio and increases in the hydrogen addition due to a reduction in the carbon amount, the cooling effect, and an increase in the OH concentration. Serbin et al. [56] analyzed the attributes of a low-emission gas turbine combustion chamber suitable for hydrogen- and natural gas-powered floating production, storage, and offloading (FPSO) vessels. A new method for simulating the pre-mixing phase of the combustion of a natural gas and hydrogen combination with an oxidizer in the radial–axial swirl channels of flame tubes is presented. The proposed hydrocarbon combustion kinetics system is utilized to conduct three-dimensional simulations for the purpose of comparing two combustion models. The topics of interest are the Finite-Rate/Eddy-Dissipation and Eddy Dissipation Concept for the annular combustion chamber of a 25 MW gas turbine engine [56]. The investigation shows that the hydrogen concentration of the mixture—which should be less than 25–30% (by volume)—determines the combustion chamber's stable working range and prevents the formation of a flashback zone in the radial–axial swirler channels as illustrated in Figure 15. The nitrogen oxide (NO) and carbon monoxide (CO) emissions from the gas turbine engines function within the limitations set by the existing environmental laws for toxic component emissions when the combustion chamber runs without a flashback zone formation within the swirler channels. Blanchard et al. [2] maintained their initial calculations for the simple and recuperative gas turbine cycles' constant power production (50 MW) and turbine outlet temperature (450 °C), as well as power production, thermal efficiency, and exergy efficiency.

Both pure hydrogen and natural gas were used as fuel sources for the basic gas turbine systems. The results showed that the efficiency of the gas turbine cycle increases when the fuel is enriched with hydrogen, based on the experimental data of most researchers [2]. As the compressor outlet temperature rose above the turbine outlet temperature, the simple gas turbine cycle outperformed the recuperative cycle in terms of efficiency above 18 bars of pressure. In terms of performance, environmental impact, and CO_2 emissions, hydrogen-fueled gas turbine cycles are more advantageous than natural gas, despite the greater cost of hydrogen per unit of power generated. The minimal fuel costs for the simple gas turbine cycle were computed as 0.345USD/kWh and 0.075USD/kWh at 20 bars when hydrogen and natural gas were utilized as fuel. For the recuperative cycle, the costs were computed as 0.322USD/kWh and 0.071USD/kWh at four-bar pressure. Cameretti et al. [57] investigated the efficiency of a 30 kW micro gas turbine combined with a solar field, utilizing two distinct gas fuels: hydrogen and a syngas produced from agricultural resources. A thermal storage

system was employed to partially meet loading needs during nighttime hours, thereby diminishing the need for fuel. A Heat Recovery Unit was also incorporated in the plant, and the whole system was simulated using the Thermoflex code. A thermodynamic analysis was carried out hourly for a given day and over 12 months, followed by an assessment of the cogeneration efficiency and energy savings. Figure 16 illustrates a comparison of the net power generated by the plant, which includes the fuel compression power, for the three fuels over time. The performance of the plant using conventional natural gas fuel is used as a benchmark for the comparison. Additionally, the CFD simulations of the combustor were conducted using the Ansys-Fluent code to evaluate the combustion development and formation of pollutant emissions, particularly NOx, with the two fuels under consideration. The results of this study provide a comprehensive understanding of the performance and emissions characteristics of the micro gas turbine plant when fueled by different gas fuels.

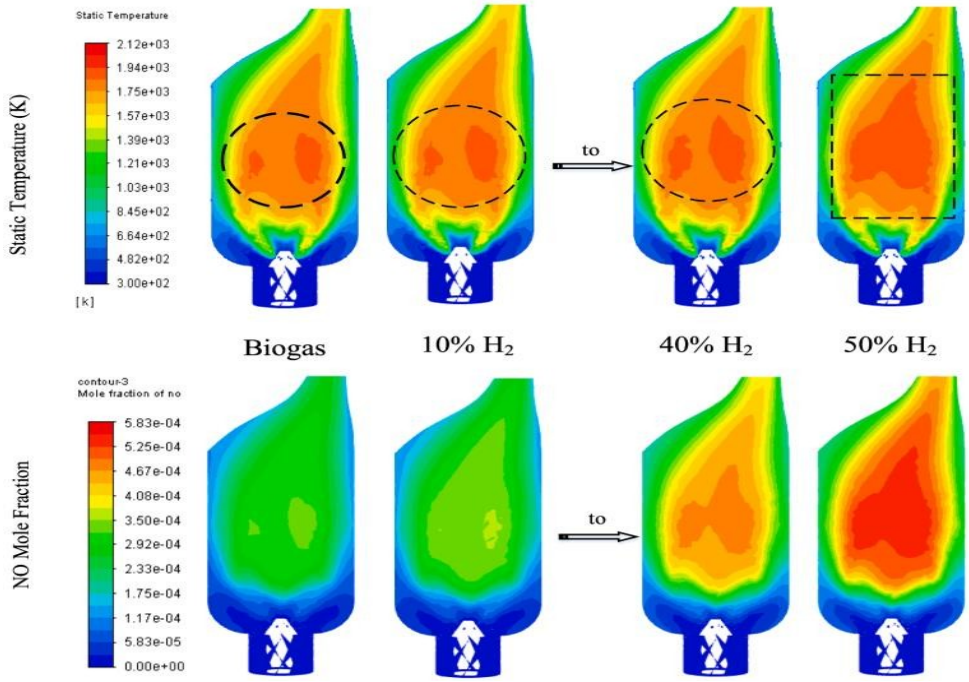

Figure 15. A sequence of images describing the biogas flame temperature distributions [K] (**above**) and NO emissions (**below**), with different rates of hydrogen concentration by Vol% [56].

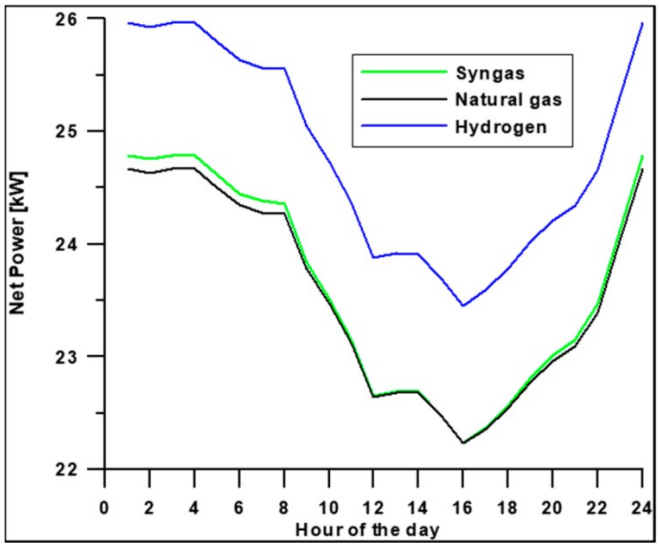

Figure 16. Net power calculated for the three fuels [57].

Nazari et al. [58] reviewed studies on hydrogen-fired gas turbines and presented a discussion of their findings. Additionally, the article puts forth recommendations for future research in this field. In Table 3, a summary of the reviewed works' principal conclusions is provided. Wang et al. [59], using CFD simulations, investigated the effect of a hydrogen additive on combustion parameters in a combustor of an aeroderivative gas turbine. The numerical model was verified using experimental data. The investigations were conducted under both constant energy input and constant mass flow rate circumstances. The results demonstrate that adding hydrogen greatly decreased the emissions of C_2H_2 and other pollutants as well as fuel residues (reductions of up to 60.9% in the fuel mass at the combustion chamber output were observed). Under constant energy input settings, the CO emissions fell as the fuel's hydrogen volume fraction grew, while under constant fuel mass flow rate conditions, they increased. The combustion mode inside the combustion chamber was changed by an excessive volume percentage of injected hydrogen, leading to both fuel-rich combustion (at a constant mass flow rate) and diffusion combustion (at a constant input power). Furthermore, as depicted in Figure 17, the introduction of hydrogen resulted in an elevation of both the pattern factor and NOx emissions at the exit of the combustion chamber. Gondal [60] studied the injection of hydrogen into a natural gas infrastructure which can have technical and energic implications. The introduction of higher concentrations of hydrogen can result in technical and energic issues in the transmission and distribution network of the natural gas infrastructure. Additionally, the components of the system, such as the compressors, are sensitive to increases in proportions of hydrogen in the natural gas mixture. Furthermore, the varying degree of acceptability for hydrogen concentrations in different elements of the natural gas infrastructure is a key consideration. For instance, compressors are the determining factor in the transmission network, with a 10% hydrogen limitation value; in contrast, the distribution network and storage elements permit a 50% hydrogen concentration. End-of-use appliances can withstand hydrogen concentrations between 20 and 50 percent. The impact of a hydrogen injection on gas quality is another important consideration. Research has indicated that introducing 2% hydrogen into the distribution network has a minimal impact, while a mixture of 10% hydrogen significantly reduces the calorific value of the supplied fuel gas below the intended amount. Figure 18 presents the statistical results of the sensitivity of hydrogen to the elements of the distribution network. In summary, the challenges and considerations for integrating hydrogen into the existing natural gas infrastructure include technical and energetic issues, the varying acceptability of hydrogen concentrations in different elements of the infrastructure, and the impact on gas quality.

Table 3. Achievements of some researchers' hydrogen fired GTs.

Reference	Type Fuel	Findings
Meziane et al. [61]	Natural gas and hydrogen	A 10% hydrogen addition to natural gas resulted in a 60% reduction in CO emissions.
Yoshimura et al. [62]	Natural gas and hydrogen	Natural gas can have its NOx emissions reduced by adding hydrogen.
Lin et al. [63]	Methane–air enriched hydrogen	A number of variables, including the equivalency ratio and hydrogen enrichment, affected the flame structure.
Medina et al. [64]	Ammonia–Hydrogen	Strong swirling flow application produced a steady flame in the combustor.
Reale et al. [65]	Methane–hydrogen	The combustion process' regularity may be enhanced by a steam injection.
Lee et al. [66]	Hydrogen and carbon monoxide	NOx emissions decreased as a result of the fuel's reduced hydrogen content.

Table 3. *Cont.*

Reference	Type Fuel	Findings
Ditaranto et al. [67]	Pure hydrogen	To avoid the emission of nitrogen oxides, exhaust gas recirculation could be substituted with nitrogen dilution of hydrogen.
Gazzani et al. [68]	Hydrogen with nitrogen and steam	Higher efficiency for diffusive flames was achieved by diluting the fuel with nitrogen.
Therkelsen et al. [69]	Hydrogen and natural gas	NO emissions decreased when the fuel/air combination was improved.
Gunasekar et al. [70]	Hydrogen and Jet A-1 fuel	Utilizing hydrogen allowed for a 10% decrease in energy efficiency.
Blanchard et al. [2]	Hydrogen and natural gas	An increase in the turbine's inlet pressure led to a decrease in the energy efficiency of a recuperated cycle and an increase in a simple cycle.
Arsalis [71]	Hydrogen and natural gas	The combustor's exergy destruction ratio decreased as the amount of hydrogen increased.
Gorgulu et al. [72]	Hydrogen	The system configuration may have an impact on how the working parameters affect energy efficiency.
Ebaid et al. [73]	Hydrogen	The design assumption affected how well a hybrid system made up of solar PVs and hydrogen GTs performed.
Cen et al. [74]	Biomass and hydrogen	Reducing carbon dioxide emissions in the intended hybrid system is achieved by using hydrogen post-firing.

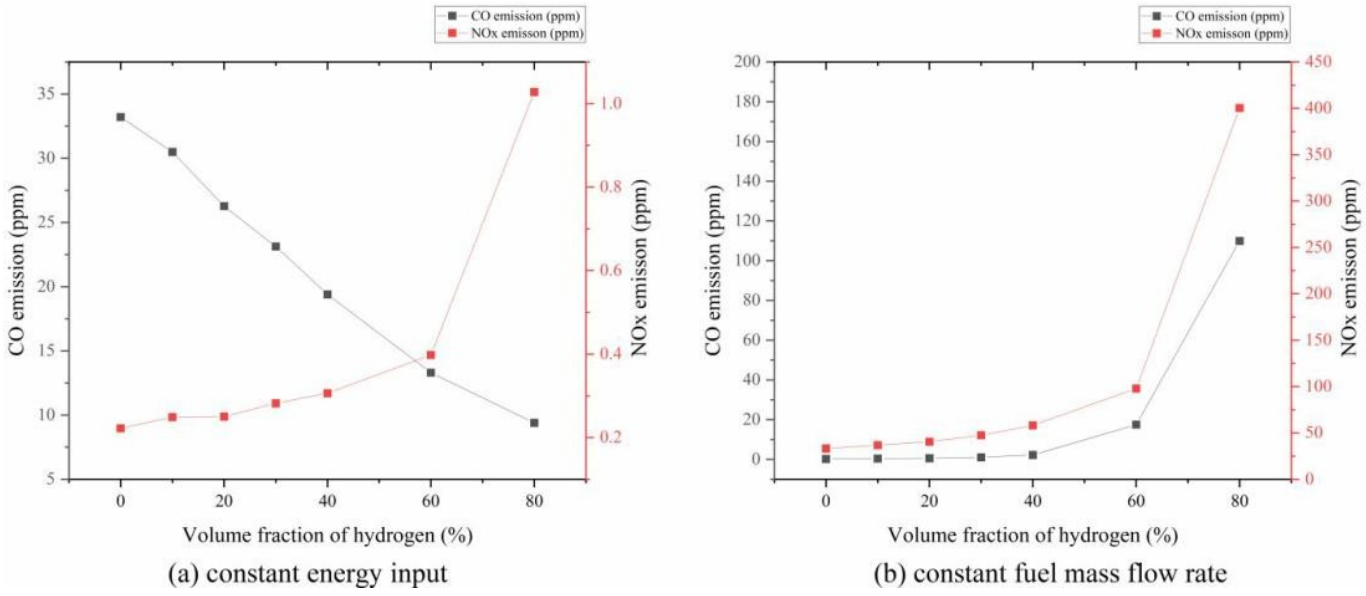

Figure 17. Emission characteristics for hydrogen–methane fuels: (**a**) constant energy input, and (**b**) constant fuel mass flow rate [59].

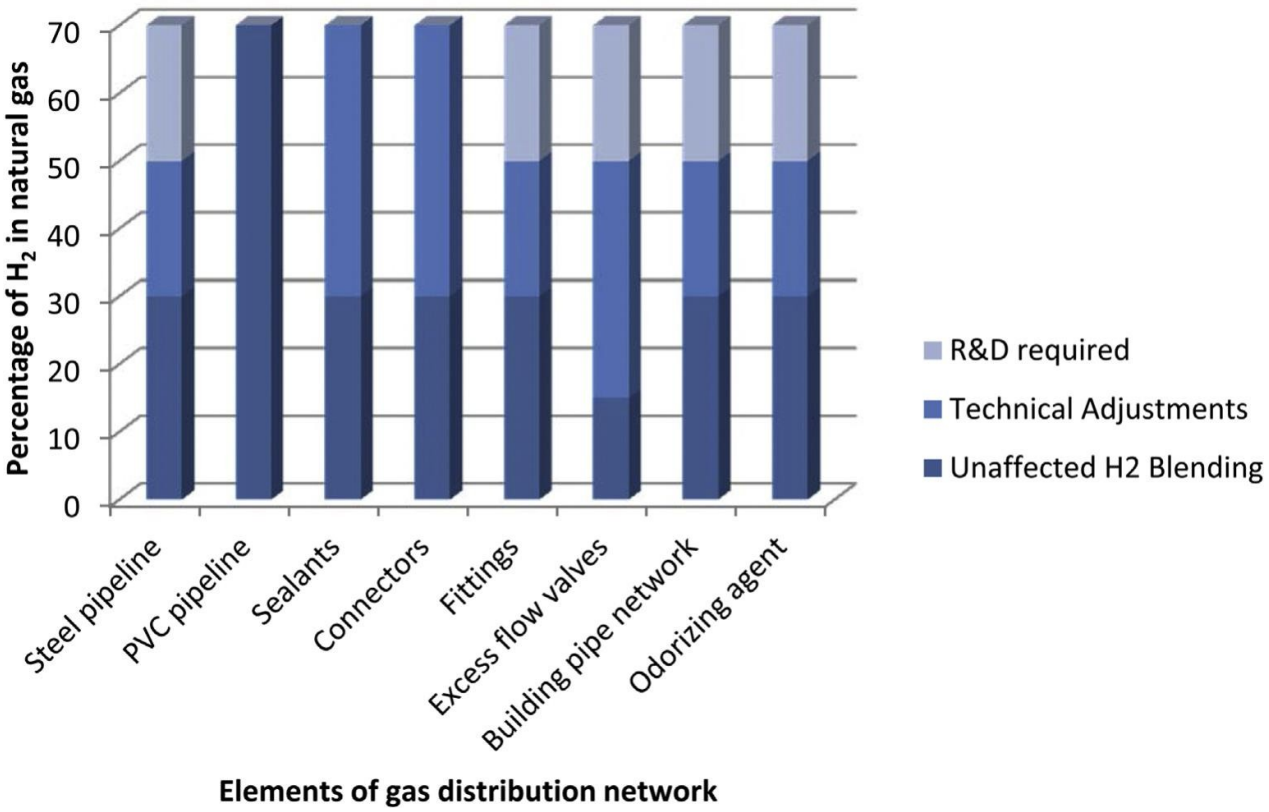

Figure 18. Hydrogen injection's sensitivity to various gas distribution network components [60].

3.3. Towards Full Hydrogen Combustion in Gas Turbines

Due to their high efficiency, fuel and operating flexibility, low emissions, high power density, and favorable economics, gas turbines are a crucial part of today's power production mix [75]. They are the cleanest type of fossil fuel power generated when operating in a combined-cycle configuration [76]. Gas turbines are used by grid operators to generate dispatchable electricity to regulate the current supply and demand because Renewable Energy Technology (RET) is intermittent. Future power systems will depend even more on improved gas turbines to meet their needs for system flexibility and energy security as installed solar and wind power generation capacity increases [77], as shown in Figure 19. Gas turbines' place in a low-carbon future depends on improved plant efficiency and carbon neutrality made possible by technological advancements in combined heat and power, massive carbon capture and storage, as well as the use of renewable fuels like hydrogen [78–80].

Oberg et al. [77], as part of the transition to future power systems in 2030, 2040, and 2050, evaluated the viability of time-shifting electricity generation employing electrolyzes, hydrogen storage, and hydrogen-fueled gas turbines using a techno-economic optimization model. The model, which covers 15 European countries, incorporates an emissions cap intended to guarantee a progressive reduction in CO_2 emissions, with the goal of reaching almost negative levels by 2050. The findings indicate that hydrogen gas turbines are crucial for managing energy output and providing capacity in a scenario where carbon emissions are limited to extremely low levels by 2050. But with energy systems that still allow significant CO_2 emissions, such as those that will exist in 2030, their competitiveness is much lower. These findings indicate that, by 2040 and 2050, the majority of investments will go toward gas turbines that are partially powered by hydrogen, with 30–77% of the hydrogen coming from biogas. However, some investments in gas turbines that are totally hydrogen-fueled are also anticipated. Investors are drawn to both open-cycle and combined-cycle gas turbines (CCGTs), and CCGTs also often appear to operate cyclically, with most start–stop cycles lasting fewer than 20 h. In comparison to burning pure natural

gas, burning pure hydrogen or hydrogen-enriched natural gas results in considerable variations in the combustion properties. Gas turbines using diffusion flame combustors may burn up to 100% hydrogen, but doing so requires pricey measures to reduce the nitrogen oxides (NOx) emissions, which makes power plants more complex and reduces their efficiency [78,81]. The current state-of-the-art low NOx operation lean premixed (LPM) combustors are typically confined to roughly 30% hydrogen by volume [82]. Due to their high fuel–air premixing levels and proximity to the lean blow-out (LBO), LPM combustors are prone to thermoacoustic instabilities [83]. Pressure oscillations, known as combustion instabilities or dynamic instabilities, occur due to the interplay between the unsteady combustion processes and acoustic waves within the combustion chamber. These instabilities have hindered the progress of LPM combustor development [84]. Research is still being conducted to develop gas turbine combustion engines that can run on any natural gas and hydrogen mixture, including hydrogen in its purest form, while still producing low NOx emissions that are on par with those of engines powered by natural gas [85]. However, operating LPM combustors with extremely high hydrogen concentrations or pure hydrogen are accompanied by a number of technical difficulties, one of which is the thermoacoustic instability characteristics of the combustor undergoing significant modifications. Tamang et al. [86] analyzed the combustion characteristics of propane fuel mixed with different amounts of hydrogen in a can-type combustor by numerical simulations. The fuel mixture's hydrogen fuel volume proportion was adjusted between 0% and 100%. The fuel's hydrogen enrichment significantly affected the flow structure, mixture fraction (lean and rich mixture side), and combustion properties, according to the results. In addition to promoting combustion, raising the flame temperature, and expanding the flammable range inside the combustor, increasing the volume fraction of hydrogen had a substantial impact on the mean mixture fraction distribution, as shown in Figure 20. Because less carbonaceous fuel was used, the use of hydrogen-enriched fuel also assisted in lowering the CO and CO_2 emissions.

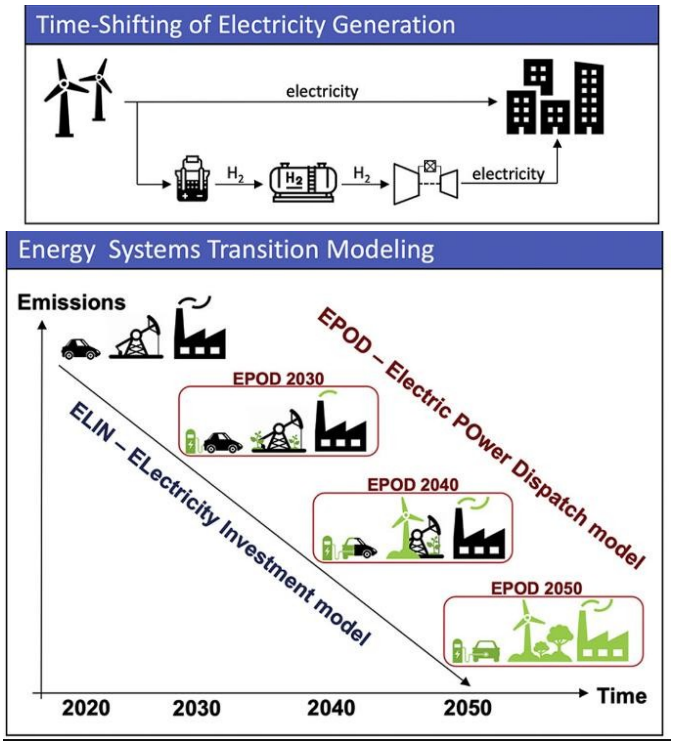

Figure 19. Hydrogen combustion in gas turbines [77].

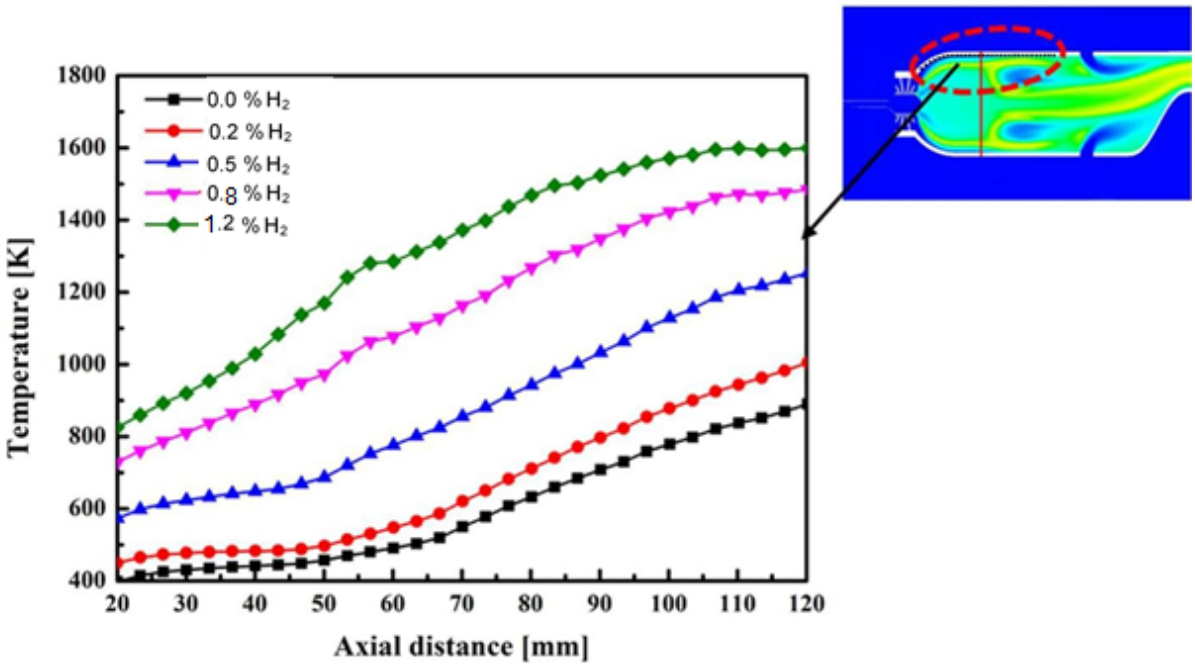

Figure 20. Effect of hydrogen addition on temperature in the combustion chamber [86].

3.4. Blending Hydrogen as Fuel in Engines

The fuel blends of gasoline and hydrogen that are best chosen for different engine operating circumstances are used in reciprocating piston hydrogen-blended gasoline engines, which are spark-ignition engines. Hydrogen is a valuable additive that helps to improve the ignition properties of hydrocarbon fuels as well as their combustion and physiochemical properties. In contrast, the performance of gasoline engines combined with hydrogen may be superior to that of conventional gasoline engines. In Rezaei et al. [87], a 2 L heavy-duty engine equipped with a single hydrogen-powered cylinder test rig was presented. The experimental findings are examined, covering changes in the engine speed, torque, ignition method, air–fuel ratio, and other aspects. This study also suggests a novel phenomenological model for hydrogen combustion prediction. The two-zone entrainment technique serves as a foundation for the model, which is enhanced by the recently created sub models tailored to hydrogen that determine the laminar flame speed and auto-ignition in the unburned mass zone. The experimental single-cylinder data are used to comprehensively validate the physical-based combustion model. Based on the complete engine calculations and experimental findings, the potentials, difficulties, and specifications for the next-generation hydrogen combustion systems are examined. Finally, this article provides insight into possible future exhaust after treatments and improvements in combustion development. Oikawa et al. [88] presented a novel method of combustion known as the Plume Ignition Combustion Concept (PCC), which entails lighting a rich mixture on fire by sparking the hydrogen jet's plume. Reducing cooling loss during combustion enhances thermal efficiency, which is important for boosting thermal efficiency in a hydrogen engine without sacrificing high power. As seen in Figure 21, PCC was added to a lean-burn regime to burn a leaner mixture worldwide in order to increase thermal efficiency and decrease NOx production. This study looked at how supercharging, which was used to recoup the leaner mixture's lower output power, affected thermal efficiency and identified the cause of the improvement.

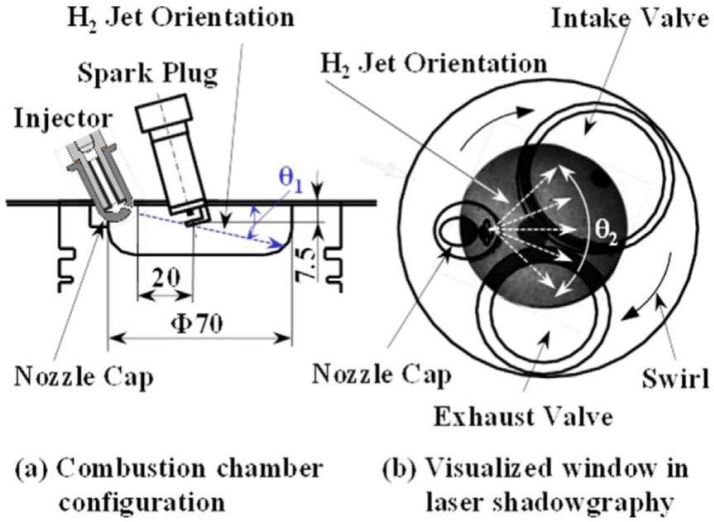

Figure 21. Setup of the combustion chamber design and organization of peripheral components. (**a**) Depicts a cross-sectional view of the combustion chamber, and (**b**) is provided to clarify the range of viewing [88].

Mariani et al. [89] reported that NOx emissions are typically higher with HCNG blends than with natural gas alone, as a result of the increased in-cylinder temperatures at a given equivalence ratio. Nonetheless, employing lean air–fuel ratios (AFR) or exhaust gas recirculation (EGR) effectively reduces NOx emissions and further boosts engine efficiency. The favorable combustion characteristics of HCNG blends also contribute to maintaining low hydrocarbon (HC) emissions. Ingo et al. [90] analyzed the maximum amount of hydrogen that can be incorporated into the natural gas grid while adhering to Euratom's guidelines. An average gas composition was determined using the most prevalent European compositions in 2021, revealing that a blend of 13.4% hydrogen with a gas mixture of 95.1% methane, 3.2% ethane, 0.7% propane, 0.3% butane, 0.3% carbon dioxide, and 0.5% nitrogen was feasible. This proposed gas composition offers engine manufacturers an indication of the hydrogen quantity that can be integrated into the gas to make it compatible with their engines. Wang et al. [91] discussed and analyzed the main achievements made by Chinese researchers in examining the effects of the hydrogen addition on engines. These primarily include various types of hydrogen-blended engines, such as gasoline, diesel, natural gas, and alcohol engines, as well as rotary engines. The focus was on engine performance, combustion, and the emission characteristics. After a thorough discussion, the advantages and disadvantages of hydrogen-blended fuel internal combustion engines were discerned and are shown in Table 4. Nevertheless, it is undeniable that gasoline and diesel will remain the predominant fuels for automobiles for the foreseeable future, indicating the considerable journey ahead before any alternative automotive fuel can achieve a widespread adoption in the market.

Shaikin et al. [92] revealed that an increase in the thickness of the near-wall unburned fuel layer, the size of slots in the combustion chamber, and the surface area of the combustion chamber contribute to reduced fuel combustion efficiency. They also showed that increasing the rate of flame propagation and decreasing the thickness of the flame front led to an improved completeness of fuel combustion. The proposed formula, which incorporates the fundamental flame propagation characteristics, enables the calculation of composite fuel combustion completeness. This suggests the formula's potential application during the design and fine-tuning phases of low-emission, energy-efficient combustion chambers in engines and power plants. Onorati et al. [93] considered the challenges associated with hydrogen ICEs, such as storage and handling, the high production costs, and the lower energy density compared to conventional fuels. Despite these challenges, hydrogen's role in future ICEs offers a promising pathway towards cleaner and more efficient

transportation systems. Zhuang et al. [94] demonstrated the complementary coordination between H_2O and H_2 in gasoline engines through experimental and simulation studies. The findings provide theoretical guidance for the development of an H_2O injection with H_2 technology to optimize combustion in gasoline engines. Figure 22 displays a comparison of the simulation and experimental results for each mechanism of the constant volume bomb. Table 5 reports the major studies by researchers on diesel and gas engines with hydrogen addition fuel.

Table 4. The advantages and disadvantages of utilizing hydrogen in gasoline and diesel engines.

Engine Type	Merits	Demerits
Gasoline engine	Reduced HC emissions, heat transfer loss, and CoV_{imep}; shortened development duration and propagation duration of flame; increased thermal efficiency; extended lean burn limit and enhanced operating stability; improved cold start and idle performance.	Reduced BMEP under high load and stoichiometric conditions; increased NOx emissions; raised CO emissions under idle conditions and stoichiometric conditions when H is too large; decreased fuel energy flow rate.
Diesel engine	Reduced regulated emissions ($CO/CO_2/HC/PM$) and unregulated emissions (alkenes/BTX/acetaldehyde/PM); increased P_{max}, heat release rate, thermal efficiency, and out power; decreased CoV_{imep}; shortened ignition delay; enhanced premixed combustion and promoted diffusion combustion.	Possible abnormal combustion; increased NOx and exhaust temperature; raised combustion noise; occasional misfire and drastic increase of $P_{max.}$

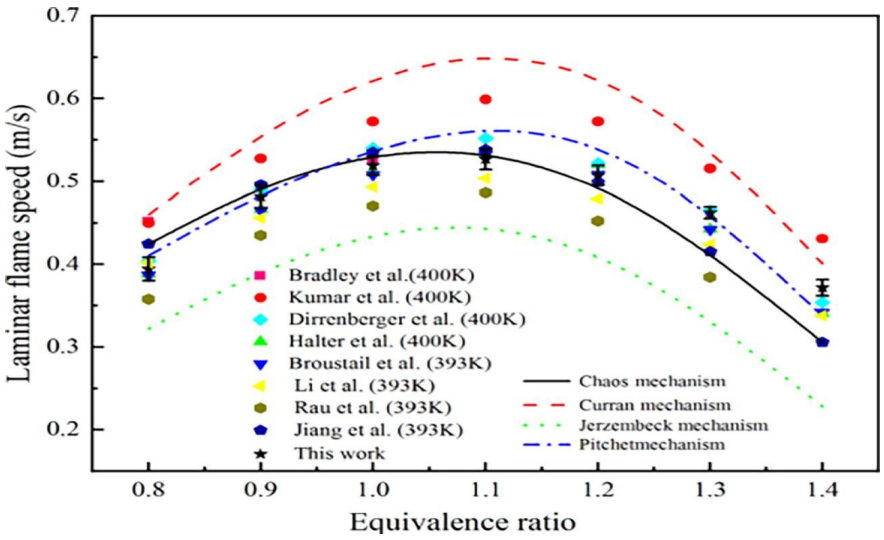

Figure 22. Laminar burning velocities of isooctane/air at different equivalence ratios [94].

Table 5. Major studies by researchers on diesel and gas engines with hydrogen addition fuel.

Author	Nature of the User	Work Condition	Processes	Hydrogen Enrichment Method and/or Amount
Yang and Liu [95]	Diesel engine supply with hydrogen addition system	Engine speed = 1200 rpm	Changed engine load, tested the emission of CO, CO_2, and HC	Addition, hydrogen for fraction = 0–7%
Zhou et al. [96]	A natural injection diesel engine	Engine speed = 1280–2560 rpm: load = 0–95%	Unregulated CO–NOx emissions and HC emissions	Hydrogen aspirated naturally, with fraction = 0–40%

Table 5. *Cont.*

Author	Nature of the User	Work Condition	Processes	Hydrogen Enrichment Method and/or Amount
Shan et al. [97]	Directly injected diesel engine, with four cylinders	Engine speed = 1500 rpm; EGR system = 0–70%	Worked with high thermal efficiency and low emissions	Hydrogen for fraction = 5–15%
Wang et al. [98]	Heavy-duty diesel engine, with six cylinders, supplied with cooler EGR and variable turbocharger	Engine speed = 1200 rpm	Nitrogen oxides, combustion process characteristics	Manifold induction H2 fraction = 0–18%
Huang and Ma [99]	Engine fueled natural gas	Engine speed = 800−2300 rpm; F/A ratio = 0.6–0.85	Multiple regression model	Hydrogen premixed with 20%
Chen et al. [100], Ma et al. [101]	A six cylinder turbocharged lean-burn heavy-duty engine	Engine speed = 1600 rpm; with loads = 0.2, 0.8, 1.4 MPa	High compression ratio, thermodynamic process, and combustion process	Hydrogen premixed with = 0–30%
Fan et al. [102]	A side-ported rotary engine fueled with natural gas–hydrogen blends	Engine speed = 2503 rpm	Mixture formation and combustion process	Hydrogen premixed with 12%
Meng et al. [103]	Four-stroke SI engine, with four cylinders, supply with the dual-injection system	Engine speed = 1500 rpm; throttle opening = 7%	Combustion and emission characteristics under lean-burn conditions	Direct injection; H2 fraction = (0–5)%.

4. Conclusions

The literature studied highlights what previous researchers have completed in the field of using hydrogen as an alternative fuel source, in different ways and uses. This is linked to several economic and environmental aspects, as hydrogen is a promising source of energy, and its production comes from various sources in nature. Due to the increasing need for power in the world, many countries have begun to invest in the power source of hydrogen, as it is considered an alternative energy source to the fossil fuels that these countries currently rely on. There are many factors affecting the hydrogen economy, including its production, storage, combustion to liberate energy, and its applications. Hydrogen production methods vary, but electrolysis and solar energy technologies remain among the most promising methods from an environmental point of view. The combustion of hydrogen enriched hydrocarbons by different type burners has been reviewed in different conditions. With an increase in the hydrogen fraction in a combustion charge, several parameters affect the hydrogen ignition time, pressure, equivalence ratio, and the chemical reaction of hydrogen with hydrocarbon.

The addition of hydrogen also significantly alters the thermal diffusivity of the light hydrocarbons in flammable mixtures, the rate of heat release, and the concentration of active radical species in the flame front, all of which contribute to the combustion speed increasing. Rich, heavy hydrocarbons suffer from thermal instability until the hydrogen is added. On the other hand, because of the thinner flame, a rise in hydrogen causes hydrodynamic instability. A hydrogen addition results in a longer lean stability limit and a more stabilized swirl burner combustion because it increases resistance to the strain rate. Furthermore, adding hydrogen reduces the CO emissions significantly without having a negative impact on the NOx emissions.

Funding: This research received no external funding.

Conflicts of Interest: The authors declare no conflict of interest.

References

1. Lieuwen, T.C.; Yang, V.; Candel, S.M. Combustion Instabilities in Gas Turbine Engines: Operational Experience, Fundamental Mechanisms, and Modeling (Progress in Astronautics and Aeronautics). *Symp. Combust.* **1992**, *24*, 1277–1296.
2. Blanchard, V.P.; Scouflaire, P.; Laux, C.O.; Ducruix, S. Combustion performance of plasma-stabilized lean flames in a gas turbine model combustor. *Appl. Energy Combust. Sci.* **2023**, *15*, 100158. [CrossRef]
3. Candel, S. Combustion dynamics and control: Progress and challenges. *Proc. Combust. Inst.* **2002**, *29*, 1–28. [CrossRef]
4. Han, J.; Jeong, J.; Cho, K.; Yu, S. Real-time combustion instability simulation with comprehensive thermo-acoustic dynamic model. *Energies* **2018**, *11*, 883. [CrossRef]
5. Zhang, B.; Ji, C.; Wang, S. Performance of a hydrogen-enriched ethanol engine at unthrottled and lean conditions. *Energy Convers. Manag.* **2016**, *114*, 68–74. [CrossRef]
6. Zhang, B.; Ji, C.; Wang, S. Combustion analysis and emissions characteristics of a hydrogen-blended methanol engine at various spark timings. *Int. J. Hydrogen Energy* **2015**, *40*, 4707–4716. [CrossRef]
7. Yuan, C.; Han, C.; Liu, Y.; He, Y.; Shao, Y.; Jian, X. Effect of hydrogen addition on the combustion and emission of a diesel free-piston engine. *Int. J. Hydrogen Energy* **2018**, *43*, 13583–13593. [CrossRef]
8. Emadi, M.; Karkow, D.; Salameh, T.; Gohil, A.; Ratner, A. Flame structure changes resulting from hydrogen-enrichment and pressurization for low-swirl premixed methane-air flames. *Int. J. Hydrogen Energy* **2012**, *37*, 10397–10404. [CrossRef]
9. Robledo, C.B.; Poorte, M.J.; Mathijssen, H.H.M.; van der Veen, R.A.C.; van Wijk, A.J.M. Fuel Cell Electric Vehicle-to-Grid Feasibility: A Technical Analysis of Aggregated Units Offering Frequency Reserves. In *Intelligent Integrated Energy Systems*; Springer: Cham, Switzerland, 2019. [CrossRef]
10. EUTurbines. The Gas Turbine Industry Commitments to Drive Europe's Transition to a Decarbonised Energy Mix. 2019. Available online: www.euturbines.eu (accessed on 28 July 2024).
11. Abdul Wahhab, H.; Aziz, A.R.A.; Al-Kayiem, H.H.; S Nasif, M. Mathematical modeling of the flow of diesel-CNG fuel mixture in a pipe under the influence of a magnetic field. *J. Appl. Fluid Mech.* **2017**, *10*, 389–396. [CrossRef]
12. Khlaf, A.M.; Ehyaei, M.A.; Wahhab, H.A.A. CFD Simulation of Premixed Flame in Counter Burner under the Influence of a Magnetic Field. *Int. J. Comput. Methods Exp. Meas.* **2023**, *11*, 233–238. [CrossRef]
13. Tang, C.; Zhang, Y.; Huang, Z. Progress in combustion investigations of hydrogen enriched hydrocarbons. *Renew. Sustain. Energy Rev.* **2014**, *30*, 195–216. [CrossRef]
14. Xie, B.; Peng, Q.; E, J.; Tu, Y.; Wei, J.; Tang, S.; Song, Y.; Fu, G. Effects of CO addition and multi-factors optimization on hydrogen/air combustion characteristics and thermal performance based on grey relational analysis. *Energy* **2022**, *255*, 124573. [CrossRef]
15. Chen, D.; Li, J.; Li, X.; Deng, L.; He, Z.; Huang, H.; Kobayashi, N. Study on combustion characteristics of hydrogen addition on ammonia flame at a porous burner. *Energy* **2023**, *263*, 125613. [CrossRef]
16. Dai, H.; Zhang, B.; Li, Z.; Wu, J. Combustion characteristics of a porous media burner with partial hydrogen injection. *Int. J. Hydrogen Energy* **2022**, *47*, 1092–1102. [CrossRef]
17. Zhang, Y.; Wu, J.; Ishizuka, S. Hydrogen addition effect on laminar burning velocity, flame temperature and flame stability of a planar and a curved CH4-H2-air premixed flame. *Int. J. Hydrogen Energy* **2009**, *34*, 519–527. [CrossRef]
18. Liu, J.; Teng, L.; Liu, B.; Han, P.; Li, W. Analysis of Hydrogen Gas Injection at Various Compositions in an Existing Natural Gas Pipeline. *Front. Energy Res.* **2021**, *9*, 685079. [CrossRef]
19. Mayrhofer, M.; Koller, M.; Seemann, P.; Prieler, R.; Hochenauer, C. Assessment of natural gas/hydrogen blends as an alternative fuel for industrial heat treatment furnaces. *Int. J. Hydrogen Energy* **2021**, *46*, 21672–21686. [CrossRef]
20. Ozturk, M.; Dincer, I. Development of renewable energy system integrated with hydrogen and natural gas subsystems for cleaner combustion. *J. Nat. Gas Sci. Eng.* **2020**, *83*, 103583. [CrossRef]
21. Miao, J.; Leung, C.W.; Cheung, C.S.; Huang, Z.H.; Zhen, H.S. Effect of hydrogen addition on overall pollutant emissions of inverse diffusion flame. *Energy* **2016**, *104*, 284–294. [CrossRef]
22. Han, W.; Dai, P.; Gou, X.; Chen, Z. A review of laminar flame speeds of hydrogen and syngas measured from propagating spherical flames. *Appl. Energy Combust. Sci.* **2020**, *1–4*, 100008. [CrossRef]
23. Ilbas, M.; Crayford, A.P.; Yilmaz, I.; Bowen, P.J.; Syred, N. Laminar-burning velocities of hydrogen-air and hydrogen-methane-air mixtures: An experimental study. *Int. J. Hydrogen Energy* **2006**, *31*, 1768–1779. [CrossRef]
24. Ma, Q.; Zhang, Q.; Chen, J.; Huang, Y.; Shi, Y. Effects of hydrogen on combustion characteristics of methane in air. *Int. J. Hydrogen Energy* **2014**, *39*, 11291–11298. [CrossRef]
25. Miao, J.; Leung, C.W.; Huang, Z.; Cheung, C.S.; Yu, H.; Xie, Y. Laminar burning velocities, Markstein lengths, and flame thickness of liquefied petroleum gas with hydrogen enrichment. *Int. J. Hydrogen Energy* **2014**, *39*, 13020–13030. [CrossRef]
26. Sun, Z.Y.; Li, G.X. Propagation characteristics of laminar spherical flames within homogeneous hydrogen-air mixtures. *Energy* **2016**, *116*, 116–127. [CrossRef]

27. Liang, W.; Wu, F.; Law, C.K. Extrapolation of laminar flame speeds from stretched flames: Role of finite flame thickness. *Proc. Combust. Inst.* **2017**, *36*, 1137–1143. [CrossRef]
28. Kim, Y.J.; Lee, B.J.; Im, H.G. Hydrodynamic and chemical scaling for blow-off dynamics of lean premixed flames stabilized on a meso-scale bluff-body. *Proc. Combust. Inst.* **2019**, *37*, 1831–1841. [CrossRef]
29. Cardona-Vargas, A.; Valencia, D.; Arrieta, C.E.; Amell, A. Combustion of a hydrogen/carbon monoxide/carbon dioxide mixture in hot and diluted streams. *J. Phys. Conf. Ser.* **2020**, *1708*, 012013. [CrossRef]
30. Mola, A.H.; Wahhab, H.A.A.; Naji, Z.H. Effects of Nozzle Diameter and Number of Carbon Atoms in Fuel on Flame Quenching in Counter Burner. In *Proceedings of the ICPER 2020: 7th International Conference on Production, Energy and Reliability*; Springer: Singapore, 2023; pp. 123–131.
31. Simon, L.; Wlodzimierz, B.; Marcin, J. Experimental study of the fuel jet combustion in high temperature and low oxygen content exhaust gases. *Energy* **2005**, *30*, 373–384. [CrossRef]
32. Khlaif, A.M.; Wahhab, H.A.A.; Ehyaei, M.A. Impact of Magnetic Field on the Stability of Laminar Flame in a Counter Burner. *Int. J. Energy Prod. Manag.* **2023**, *8*, 229–234.
33. Mihăescu, L.; Stanciu, D.; Lăzăroiu, G.; Pîșă, I.; Negreanu, G. Comparative analysis between methane and hydrogen regarding ignition and combustion in diffusive mode. In Proceedings of the E3S Web Conference, Sozopol, Bulgaria, 18–21 September 2021; EDP Sciences: Les Ulis, France, 2021; Volume 327. [CrossRef]
34. Vance, F.H.; Shoshin, Y.; de Goey, P.; van Oijen, J. Flame stabilization and blow- off of ultra-lean H2-air premixed flames. *Energies* **2021**, *14*, 1977. [CrossRef]
35. Mitu, M.; Razus, D.; Schroeder, V. Laminar burning velocities of hydrogen-blended methane—Air and natural gas air mixture, calculated from the early stage of p(t) records in a spherical. *Energies* **2021**, *14*, 7556. [CrossRef]
36. Raman, K. *Laminar Burning Velocities of Lean Hydrogen-Air Mixtures*; Explosion Dynamics Laboratory Report FM97-15; California Institute of Technology: Pasadena, CA, USA, 1998; Volume 149, pp. 162–172.
37. Ren, F.; Chu, H.; Xiang, L.; Han, W.; Gu, M. Effect of hydrogen addition on the laminar premixed combustion characteristics the main components of natural gas. *J. Energy Inst.* **2019**, *92*, 1178–1190. [CrossRef]
38. Wei, J.; Fu, G.; Yang, W.; Li, S.; E, J.; Peng, Q.; Zhang, A. Investigation on hydrogen-fueled combustion characteristics and thermal performance in a micro heat-recirculation combustor inserted with block. *Int. J. Hydrogen Energy* **2021**, *46*, 36515–36527. [CrossRef]
39. Tan, Y.; E, J.; Chen, J.; Liao, G.; Zhang, F.; Li, J. Investigation on combustion characteristics and thermal performance of a three rearward-step structure micro combustor fueled by premixed hydrogen/air. *Renew. Energy* **2022**, *186*, 486–504. [CrossRef]
40. Peng, Q.; Wei, J.; Yang, W.; E, J. Study on combustion characteristic of premixed H2/C3H8/air and working performance in the micro combustor with block. *Fuel* **2022**, *318*, 123676. [CrossRef]
41. Shi, Z.; Li, W.; Wei, J.; Xie, B.; Kang, Z.; Fu, G.; Peng, Q. Effects of dual-inlet on premixed hydrogen/air combustion characteristics and thermal performance for micro thermophotovoltaic application. *Int. J. Hydrogen Energy* **2022**, *47*, 33872–33882. [CrossRef]
42. Yilmaz, H.; Karyeyen, S.; Tepe, A.Ü.; Brüggemann, D. Colorless distributed combustion characteristics of hydrogen/air mixtures in a micro combustor. *Fuel* **2023**, *332*, 126163. [CrossRef]
43. Barati, S.; De Santoli, L.; Basso, G.L. Modeling and Analysis of a Micro Gas Turbine Fuelled with Hydrogen and Natural Gas Blends. In Proceedings of the E3S Web Conference, Rome, Italy, 15–17 September 2021; EDP Sciences: Les Ulis, France, 2021; Volume 312, pp. 1–13. [CrossRef]
44. Brauers, H.; Richter, P. *The Paris Climate Agreement: Is It Suffi cient to Limit Climate Change?* DIW Roundup: Berlin, Germany, 2016; pp. 1–7.
45. Khan, M.I.; Al-Ghamdi, S.G. Hydrogen economy for sustainable development in GCC countries: A SWOT analysis considering current situation, challenges, and prospects. *Int. J. Hydrogen Energy* **2023**, *48*, 10315–10344. [CrossRef]
46. Griffiths, S.; Sovacool, B.K.; Kim, J.; Bazilian, M.; Uratani, J.M. Industrial decarbonization via hydrogen: A critical and systematic review of developments, socio- technical systems and policy options. *Energy Res. Soc. Sci.* **2021**, *80*, 102208. [CrossRef]
47. Menéndez-Agudin, A.; Rocca, R.; Fernandez, G.; Luengo-Baranguan, L.; Zaldivar, D. Hydrogen Technologies to Provide Flexibility to the Electric System: A Review. *Renew. Energy Power Qual. J.* **2022**, *20*, 656–661. [CrossRef]
48. Sánchez, A.; Zhang, Q.; Martín, M.; Vega, P. Towards a new renewable power system using energy storage: An economic and social analysis. *Energy Convers. Manag.* **2022**, *252*, 115056. [CrossRef]
49. Marouani, I.; Guesmi, T.; Alshammari, B.M.; Alqunun, K.; Alzamil, A.; Alturki, M.; Abdallah, H.H. Integration of Renewable-Energy-Based Green Hydrogen into the Energy Future. *Processes* **2023**, *11*, 2685. [CrossRef]
50. Ozturk, M.; Midilli, A.; Dincer, I. Effective use of hydrogen sulfide and natural gas resources available in the Black Sea for hydrogen economy. *Int. J. Hydrogen Energy* **2021**, *46*, 10697–10707. [CrossRef]
51. Olabi, A.G.; Bahri, A.S.; Abdelghafar, A.A.; Baroutaji, A.; Sayed, E.T.; Alami, A.H.; Rezk, H.; Abdelkareem, M.A. Large-vscale hydrogen production and storage technologies: Current status and future directions. *Int. J. Hydrogen Energy* **2021**, *46*, 23498–23528. [CrossRef]
52. Qazi, U.Y. Future of Hydrogen as an Alternative Fuel for. *Energies* **2022**, *15*, 4741. [CrossRef]
53. IEA. *The Future of Hydrogen for G20. Seizing Today's Opportunities*; Rep. Prep. By IEAG20; IEA: Tokyo, Japan, 2019; Volume 6, pp. 246–256. Available online: https://www.iea.org/reports/the-future-of-hydrogen (accessed on 28 July 2024).
54. Rosen, M.A.; Koohi-Fayegh, S. The prospects for hydrogen as an energy carrier: An overview of hydrogen energy and hydrogen energy systems. *Energy Ecol. Environ.* **2016**, *1*, 10–29. [CrossRef]

55. Benaissa, S.; Adouane, B.; Ali, S.M.; Rashwan, S.S.; Aouachria, Z. Investigation on combustion characteristics and emissions of biogas/hydrogen blends in gas turbine combustors. *Therm. Sci. Eng. Prog.* **2022**, *27*, 101178. [CrossRef]
56. Serbin, S.; Burunsuz, K.; Chen, D.; Kowalski, J. Investigation of the Characteristics of a Low-Emission Gas Turbine Combustion Chamber Operating on a Mixture of Natural Gas and Hydrogen. *Pol. Marit. Res.* **2022**, *29*, 64–76. [CrossRef]
57. Cameretti, M.C.; Cappiello, A.; de Robbio, R.; Tuccillo, R. Comparison between hydrogen and syngas fuels in an integrated micro gas turbine/solar field with storage. *Energies* **2020**, *13*, 4764. [CrossRef]
58. Nazari, M.A.; Alavi, M.F.; Salem, M.; Assad, M.E.H. Utilization of hydrogen in gas turbines: A comprehensive review. *Int. J. Low-Carbon Technol.* **2022**, *17*, 513–519. [CrossRef]
59. Wang, K.; Li, F.; Zhou, T.; Ao, Y. Numerical Study of Combustion and Emission Characteristics for Hydrogen Mixed Fuel in the Methane-Fueled Gas Turbine Combustor. *Aerospace* **2023**, *10*, 72. [CrossRef]
60. Gondal, I.A. Hydrogen integration in power-to-gas networks. *Int. J. Hydrogen Energy* **2019**, *44*, 1803–1815. [CrossRef]
61. Meziane, S.; Bentebbiche, A. Numerical study of blended fuel natural gas-hydrogen combustion in rich/quench/lean combustor of a micro gas turbine. *Int. J. Hydrogen Energy* **2019**, *44*, 15610–15621. [CrossRef]
62. Yoshimura, T.; McDonell, V.; Samuelsen, S. Evaluation of Hydrogen Addition to Natural Gas on the Stability and Emissions Behavior of a Model Gas Turbine Combustor. In *Turbo Expo: Power for Land, Sea, and Air*; The American Society of Mechanical Engineers: Tokyo, Japan, 2008; pp. 573–581.
63. Liu, X.; Bertsch, M.; Subash, A.A.; Yu, S.; Szasz, R.-Z.; Li, Z.; Petersson, P.; Bai, X.-S.; Aldén, M.; Lörstad, D. Investigation of turbulent premixed methane/air and hydrogen-enriched methane/air flames in a laboratory-scale gas turbine model combustor. *Int. J. Hydrogen Energy* **2021**, *46*, 13377–13388. [CrossRef]
64. Valera-Medina, A.; Morris, S.; Runyon, J.; Pugh, D.; Marsh, R.; Beasley, P.; Hughes, T. Ammonia, Methane and Hydrogen for Gas Turbines. *Energy Procedia* **2015**, *75*, 118–123. [CrossRef]
65. Reale, F.; Sannino, R. Water and steam injection in micro gas turbine supplied by hydrogen enriched fuels: Numerical investigation and performance analysis. *Int. J. Hydrogen Energy* **2021**, *46*, 24366–24381. [CrossRef]
66. Lee, M.C.; Seo, S.B.; Chung, J.H.; Kim, S.M.; Joo, Y.J.; Ahn, D.H. Gas turbine combustion performance test of hydrogen and carbon monoxide synthetic gas. *Fuel* **2010**, *89*, 1485–1491. [CrossRef]
67. Ditaranto, M.; Li, H.; Hu, Y. Evaluation of a pre-combustion capture cycle based on hydrogen fired gas turbine with exhaust gas recirculation (EGR). *Energy Procedia* **2014**, *63*, 1972–1975. [CrossRef]
68. Gazzani, M.; Chiesa, P.; Martelli, E.; Sigali, S.; Brunetti, I. Using hydrogen as gas turbine fuel: Premixed versus diffusive flame combustors. *J. Eng. Gas Turbines Power* **2014**, *136*, 051504. [CrossRef]
69. Therkelsen, P.; Werts, T.; McDonell, V.; Samuelsen, S. Analysis of nox formation in a hydrogen fueled gas turbine engine. In Proceedings of the ASME Turbo Expo 2008: Power for Land, Sea, and Air. Volume 3: Combustion, Fuels and Emissions, Parts A and B, Berlin, Germany, 9–13 June 2008; Volume 3, pp. 653–664. [CrossRef]
70. Gunasekar, P.; Manigandan, S.; Venkatesh, S.; Gokulnath, R.; Vimal, R.; Boomadevi, P. Effect of hydrogen addition on exergetic performance of gas turbine engine. *Aircr. Eng. Aerosp. Technol.* **2020**, *92*, 180–185. [CrossRef]
71. Arsalis, A. Thermodynamic modeling and parametric study of a small-scale natural gas/hydrogen-fueled gas turbine system for decentralized applications. *Sustain. Energy Technol. Assess.* **2019**, *36*, 100560. [CrossRef]
72. Görgülü, A.; Yağlı, H.; Koç, Y.; Koç, A. Comprehensive analysis of the effect of water injection on performance and emission parameters of the hydrogen fuelled recuperative and non-recuperative gas turbine system. *Int. J. Hydrogen Energy* **2020**, *45*, 34254–34267. [CrossRef]
73. Ebaid, M.S.Y.; Hammad, M.; Alghamdi, T. THERMO economic analysis OF PV and hydrogen gas turbine hybrid power plant of 100 MW power output. *Int. J. Hydrogen Energy* **2015**, *40*, 12120–12143. [CrossRef]
74. Cen, S.; Li, K.; Liu, Q.; Jiang, Y. Solar energy-based hydrogen production and post- firing in a biomass fueled gas turbine for power generation enhancement and carbon dioxide emission reduction. *Energy Convers. Manag.* **2021**, *233*, 113941. [CrossRef]
75. Jansohn, P. Overview of gas turbine types and applications. In *Modern Gas Turbine Systems, High Efficiency, Low Emission, Fuel Flexible Power Generation*; Woodhead Publishing: Cambridge, UK, 2013; pp. 21–43. [CrossRef]
76. Javadi, M.A.; Najafi, N.J.; Abhari, M.K.; Jabery, R.; Pourtaba, H. 4E analysis of three different configurations of a combined cycle power plant integrated with a solar power tower system. *Sustain. Energy Technol. Assess.* **2021**, *48*, 101599. [CrossRef]
77. Öberg, S.; Odenberger, M.; Johnsson, F. Exploring the competitiveness of hydrogen- fueled gas turbines in future energy systems. *Int. J. Hydrogen Energy* **2022**, *47*, 624–644. [CrossRef]
78. Akroot, A.; Ekici, Ö.; Köksal, M. Process modeling of an automotive pem fuel cell system. *Int. J. Green Energy* **2019**, *16*, 778–788. [CrossRef]
79. Akroot, A.; Nadeesh, A. Performance Analysis of Hybrid Solid Oxide Fuel Cell-Gas Turbine Power System. *Int. J. Eng. Sci.* **2021**, *9*, 43–51.
80. Guilbert, D.; Vitale, G. Hydrogen as a Clean and Sustainable Energy Vector for Global Transition from Fossil-Based to Zero-Carbon. *Clean Technol.* **2021**, *3*, 881–909. [CrossRef]
81. Ditaranto, M.; Heggset, T.; Berstad, D. Concept of hydrogen fired gas turbine cycle with exhaust gas recirculation: Assessment of process performance. *Energy* **2020**, *192*, 116646. [CrossRef]
82. Cecere, D.; Giacomazzi, E.; Di Nardo, A.; Calchetti, G. Gas Turbine Combustion Technologies for Hydrogen Blends. *Energies* **2023**, *16*, 6829. [CrossRef]

83. De Giorgi, M.G.; Campilongo, S.; Ficarella, A.; De Falco, G.; Commodo, M.; D'Anna, A. Pollutant formation during the occurrence of flame instabilities under very- lean combustion conditions in a liquid-fuel burner. *Energies* **2017**, *10*, 352. [CrossRef]
84. Miniero, L. Reactive Flows Dynamics for Low-Emissions Aviation: Spray Combustion in Hot Vitiated Environment and Passive Control of Thermoacoustic Instabilities. Ph.D. Thesis, ETH Zurich, Zurich, Switzerland, 2023.
85. Hwang, J.; Maharjan, K.; Cho, H.J. A review of hydrogen utilization in power generation and transportation sectors: Achievements and future challenges. *Int. J. Hydrogen Energy* **2023**, *48*, 28629–28648. [CrossRef]
86. Tamang, S.; Park, H. Numerical investigation of combustion characteristics for hydrogen mixed fuel in a can-type model of the gas turbine combustor. *Int. J. Hydrogen Energy* **2023**, *48*, 11493–11512. [CrossRef]
87. Rezaei, R.; Hayduk, C.; Fandakov, A.; Rieß, M.; Sens, M.; Delebinski, T.O. *Numerical and Experimental Investigations of Hydrogen Combustion for Heavy-Duty Applications*; SAE Technical Paper; SAE International: Warrendale, PA, USA, 2021. [CrossRef]
88. Oikawa, M.; Kojiya, Y.; Sato, R.; Goma, K.; Takagi, Y.; Mihara, Y. Effect of supercharging on improving thermal efficiency and modifying combustion characteristics in lean-burn direct-injection near-zero-emission hydrogen engines. *Int. J. Hydrogen Energy* **2022**, *47*, 1319–1327. [CrossRef]
89. Mariani, A.; Morrone, B.; Unich, A. A Review of Hydrogen-Natural Gas Blend Fuels in Internal Combustion Engines. *Foss. Fuel Environ.* **2012**, *2*, 17–36. [CrossRef]
90. Ingo, C.; Tuuf, J.; Björklund-Sänkiaho, M. Impact of Hydrogen on Natural Gas Compositions to Meet Engine Gas Quality Requirements. *Energies* **2022**, *15*, 7990. [CrossRef]
91. Wang, L.; Hong, C.; Li, X.; Yang, Z.; Guo, S.; Li, Q. Review on blended hydrogen- fuel internal combustion engines: A case study for China. *Energy Rep.* **2022**, *8*, 6480–6498. [CrossRef]
92. Shaikin, A.P.; Galiev, I.R.; Epishkin, V.E. Influence flame speed and flame thickness on completeness of combustion hythane. In *IOP Conference Series: Materials Science and Engineering 2020*; IOP Publishing: Bristol, UK, 2020; Volume 734. [CrossRef]
93. Onorati, A.; Payri, R.; Vaglieco, B.; Agarwal, A.; Bae, C.; Bruneaux, G.; Canakci, M.; Gavaises, M.; Günthner, M.; Hasse, C.; et al. The role of hydrogen for future internal combustion engines. *Int. J. Engine Res.* **2022**, *23*, 529–540. [CrossRef]
94. Zhuang, Y.; Gao, C.; Zhai, R.; Wu, R. Study of water and hydrogen addition on the pyrolysis and combustion characteristics of isooctane. *Fuel* **2023**, *334*, 126662. [CrossRef]
95. Yang, Z.Z.; Li, H. Effects of H2 addition on exhaust emissions of CO, CO2 and HC in cummins ISM370 diesel engine. *Acta Armamentarii* **2015**, *36*, 40–45. [CrossRef]
96. Zhou, J.H.; Cheung, C.S.; Zhao, W.Z.; Leung, C.W. Diesel-hydrogen dual-fuel combustion and its impact on unregulated gaseous emissions and particulate emissions under different engine loads and engine speeds. *Energy* **2016**, *94*, 110–123. [CrossRef]
97. Shan, X.; Qian, Y.; Zhu, L.; Lu, X. Effects of EGR rate and hydrogen/carbon monoxide ratio on combustion and emission characteristics of biogas/diesel dual fuel combustion engine. *Fuel* **2016**, *181*, 1050–1057. [CrossRef]
98. Wang, L.; Liu, D.; Yang, Z.; Li, H.; Wei, L.; Li, Q. Effect of H2 addition on combustion and exhaust emissions in a heavy-duty diesel engine with EGR. *Int. J. Hydrogen Energy* **2018**, *43*, 22658–22668. [CrossRef]
99. Huang, Y.; Ma, F. Intelligent regression algorithm study based on performance and NOx emission experimental data of a hydrogen enriched natural gas engine. *Int. J. Hydrogen Energy* **2016**, *41*, 11308–11320. [CrossRef]
100. Chen, Z.; Xu, B.; Zhang, F.; Liu, J. Quantitative research on thermodynamic process and efficiency of a LNG heavy-duty engine with high compression ratio and hydrogen enrichment. *Appl. Therm. Eng.* **2017**, *125*, 1103–1113. [CrossRef]
101. Ma, F.; Wang, M.; Jiang, L.; Chen, R.; Deng, J.; Naeve, N.; Zhao, S. Performance and emission characteristics of a turbocharged CNG engine fueled by hydrogen-enriched compressed natural gas with high hydrogen ratio. *Int. J. Hydrogen Energy* **2010**, *35*, 6438–6447. [CrossRef]
102. Fan, B.; Pan, J.; Liu, Y.; Zhu, Y.; Pan, Z.; Chen, W.; Otchere, P. Effect of hydrogen injection strategies on mixture formation and combustion process in a hydrogen direct injection plus natural gas port injection rotary engine. *Energy Convers. Manag.* **2018**, *160*, 150–164. [CrossRef]
103. Meng, F.; Yu, X.; He, L.; Liu, Y.; Wang, Y. Study on combustion and emission characteristics of a n-butanol engine with hydrogen direct injection under lean burn conditions. *Int. J. Hydrogen Energy* **2018**, *43*, 7550–7561. [CrossRef]

Disclaimer/Publisher's Note: The statements, opinions and data contained in all publications are solely those of the individual author(s) and contributor(s) and not of MDPI and/or the editor(s). MDPI and/or the editor(s) disclaim responsibility for any injury to people or property resulting from any ideas, methods, instructions or products referred to in the content.